



Minerva Access is the Institutional Repository of The University of Melbourne

Author/s:

Wasko, C;Shao, Y;Vogel, E;Wilson, L;Wang, QJ;Frost, A;Donnelly, C

Title:

Understanding trends in hydrologic extremes across Australia

Date:

2021-02-01

Citation:

Wasko, C., Shao, Y., Vogel, E., Wilson, L., Wang, Q. J., Frost, A. & Donnelly, C. (2021).
Understanding trends in hydrologic extremes across Australia. *Journal of Hydrology*, 593,
<https://doi.org/10.1016/j.jhydrol.2020.125877>.

Persistent Link:

<https://hdl.handle.net/11343/264214>

1 **Understanding trends in hydrologic extremes across Australia**

2 Conrad Wasko^{1*}, Yawen Shao¹, Elisabeth Vogel², Louise Wilson², QJ Wang¹, Andrew Frost³, Chantal
3 Donnelly⁴

4 ¹Department of Infrastructure Engineering, The University of Melbourne, Parkville, Australia

5 ²Australian Bureau of Meteorology, Melbourne, Australia

6 ³Australian Bureau of Meteorology, Sydney, Australia

7 ⁴Australian Bureau of Meteorology, Brisbane, Australia

8 [*conrad.wasko@unimelb.edu.au](mailto:conrad.wasko@unimelb.edu.au)

9 **Key points:**

10 # Australian Landscape Water Balance model is used to evaluate hydrologic trends

11 # Trends in modelled streamflow are evaluated against observed streamflow

12 # Rainfall, soil moisture, and streamflow trends are consistent with tropical expansion

13 # Changes in flood and drought are linked to mean rainfall changes at continental scale

14 # Trends are more likely to be driven by local factors at the catchment scale

15 **Key words:**

16 Australia, rainfall, runoff, soil moisture, drought, flood, climate change, trend, AWRA-L

17

18 **Abstract**

19 Changes in the hydrologic cycle have far reaching impacts on agricultural productivity, water resources
20 availability, riverine ecosystems, and our ability to manage environmental assets, bushfire risk, and flood
21 hazard. For example, declining rainfall in the southeast of Australia has led to a prolonged period of
22 drought, with serious impacts on agriculture, the environment, and water supply to urban and rural
23 towns. Here, using the continental wide Australian Water Resources Assessment Landscape model
24 (AWRA-L), we evaluate historical trends from 1960 to 2017 in rainfall, soil moisture, evapotranspiration,
25 and runoff to explain changing drought and flooding. Northern parts of Australia have experienced
26 increasing annual rainfall totals, resulting in increased water availability in the tropics with increased soil
27 moisture, evapotranspiration, and runoff, particularly during the hot, wet monsoon season. In contrast,
28 the southwest and southeast coast of Australia have experienced declines in rainfall, particularly in the
29 colder months, corresponding with decreasing evapotranspiration, soil moisture, and runoff. Trends in
30 flooding are aligned with runoff trends, and closely follow trends in rainfall, with changes in soil moisture
31 of secondary influence. Streamflow droughts, measured by the standardised runoff index, are increasing
32 across large parts of Australia, with these increases more widespread than changes in rainfall alone.
33 Increases in rainfall in the tropics of northern Australia appear to be related to decreasing drought
34 occurrence and extent, but this trend is not universal, suggesting changes in rainfall alone are not an
35 indicator of changing drought conditions.

36 **1 Introduction**

37 **1.1 Changes in the global hydrological cycle**

38 One of the most important questions in hydrology is how the hydrologic cycle is being impacted by climate
39 change (Huntington, 2006; Koutsoyiannis, 2020). Water in the landscape and rivers is essential for:
40 agriculture, town and industrial water supply, the environment, cultural values, recreation, hydropower
41 and more; hence changes to when and where water is available has far reaching impacts. In terms of
42 hydrologic extremes, flood and droughts are among the costliest natural disasters in the world, causing
43 risk to life, food security and, in the case of drought, increased bushfire risk.

44 Globally, precipitation has increased as per energy constraints (Allan et al., 2020; Allen and Ingram, 2002)
45 at approximately 2.4mm/decade (Becker et al., 2013; Hartmann et al., 2013) in line with climate model
46 projections of a 2% increase in precipitation per degree increase in global mean temperature (Kharin et
47 al., 2013). Most of the increases in precipitation have occurred over tropical areas with decreases
48 elsewhere (Beck et al., 2019), while precipitation extremes such as annual maxima of daily rainfall have
49 increased universally at a rate close to 7% per degree increase in global mean temperature (Sun et al.,
50 2020; Westra et al., 2013). There is evidence that, consistent with changes in rainfall, soil moisture has
51 experienced wetting trends in the tropics and drying trends in the extra tropics (Feng and Zhang, 2015;
52 Liu et al., 2019) but trends differ depending on the data set used (Albergel et al., 2013).

53 Compared to changes in annual average conditions, changes in hydrological extremes are more
54 challenging to quantify and understand. Increasing temperatures have increased the likelihood of drought
55 conditions in many regions of the world (Hartmann et al., 2013; Liu et al., 2019), though again, results
56 differ depending on the index used (Asadi Zarch et al., 2015). Despite many studies pointing to increases
57 in extreme precipitation (Donat et al., 2013; Groisman et al., 2005; Martinez-Villalobos and Neelin, 2018;
58 Sun et al., 2020; Westra et al., 2013), there is a very mixed trend in flood response (Sharma et al., 2018)
59 with more sites globally showing decreases in flooding than increases (Do et al., 2017). Despite this
60 variability, trends in high flows follow average annual flow trends both globally (Gudmundsson et al.,
61 2019) and across Australia (Zhang et al., 2016). In regions free of snow-melt, it has been postulated that
62 changes in flooding are due to changing antecedent soil moisture conditions (Ivancic and Shaw, 2015;
63 Sharma et al., 2018; Wasko et al., 2019). However, few studies have studied trends in antecedent
64 conditions explicitly (Tramblay et al., 2019; Wasko and Nathan, 2019a).

65 **1.2 Hydrological trends in Australia**

66 Australia forms a valuable test case for investigating the impacts of climate change on the hydrologic cycle.
67 It straddles the tropics and extratropics, experiencing a wide range of climates, and is largely free of
68 snowmelt. In addition, trends in Australian precipitation and temperature reflect global patterns
69 (Alexander et al., 2007), although streamflow exhibits extremely high variability compared to the rest of
70 the world (Chiew and McMahon, 2002; McMahon et al., 2007; Peel et al., 2004).

71 Mean annual rainfall has increased in the tropical north of Australia and decreased in the south (Dey et
72 al., 2019), particularly along the south-east and south-west coasts due to changed cutoffs and frontal
73 systems (Risbey et al., 2013) consistent with a tropical expansion (Grise et al., 2018; Staten et al., 2018).
74 For example, south-western Australia has undergone decreased cool season rainfall in April to October,
75 with sharp decreases in May-July rainfall since 1970. There has been a similar decline of rainfall over
76 south-eastern Australia in April to October rainfall since the late 1990s. Meanwhile, in northern Australia,
77 there has been an observed rainfall increase since the 1970s, especially in the northwest (CSIRO & BOM,
78 2018).

79 Since the 1950s increasing streamflow in the northern tropics and decreasing streamflow over southern
80 Australia has been observed (Zhang et al., 2016). Across Australia studies of trends in evapotranspiration
81 show mixed trends temporally and spatially. Prior to 1999, decreasing trends in observed pan evaporation
82 across Australia were linked to declining wind speeds (Johnson and Sharma, 2010), but since then, many
83 sites have shown increased pan evaporation, possibly due to an increased vapor pressure deficit (Stephens
84 et al., 2018). Despite increases in global estimates of terrestrial evapotranspiration (Zeng et al., 2018),
85 evapotranspiration estimates derived from remote sensing and flux towers show a decrease in
86 evapotranspiration between 1998-2008 attributed to moisture limitations (Jung et al., 2010).

87 There is a large discrepancy in trends calculated between different soil moisture products, but in general
88 datasets point to more severe droughts in arid and semi-arid regions (Liu et al., 2019). Using data obtained
89 from the European Space Agency, soil moisture was found to be decreasing across Australia between 1979
90 and 2013, with the exception of the tropical north (Feng and Zhang, 2015). However, another study for
91 1988–2010 using multiple reanalysis and satellite derived data sets indicated largely conflicting results
92 between data sets, particularly at the regional scale (Albergel et al., 2013). This may be because reanalysis
93 data sets, particularly ERA-INTERIM, have large rainfall biases (Andersson et al., 2015; Weedon et al.,
94 2014) while remote sensed data sets measure soil moisture at different depths (Holgate et al., 2016).

95 The magnitude of extreme hourly and daily rainfall, across a range of exceedance thresholds, has
96 increased over the last half a century across Australia (Alexander and Arblaster, 2017; Guerreiro et al.,
97 2018) with shifts to a greater frequency of longer duration events in the tropics and shorter duration
98 events in extra-tropics (Dey et al., 2020). Despite more evidence for increasing rainfall extremes compared
99 to decreases, more streamflow gauging sites show decreases in annual maxima than increases (Ishak et
100 al., 2013; Zhang et al., 2016). Decreased flooding has been attributed to decreased antecedent soil
101 moisture prior to the onset of the storm events across southern parts of Australia (Wasko and Nathan,
102 2019a). This demonstrates how a better understanding of the drivers of changes on streamflow and
103 flooding, that is, rainfall, evapotranspiration and soil moisture, and how they interact, is required to better
104 predict the likely impacts of climate change on the hydrological cycle, and subsequently economic activity,
105 the environment, communities, and ecosystems (Berghuijs et al., 2019).

106 **1.3 Research gap in understanding drivers of concurrent hydrological trends**

107 Due to the greater number of rainfall gauging stations and observations compared to streamflow, studies
108 often infer impacts to flooding from changes in rainfall. However, this approach may lead to apparent
109 contradictions such as increasing rainfall extremes which are not associated with increased flooding
110 (Sharma et al., 2018). Few studies examine hydroclimatic variables in unison (exceptions include, Johnson
111 et al., 2016; Wasko et al., 2020; Wasko and Nathan, 2019a) and of those that do, most focus on
112 instrumented catchments and the Millennium Drought (2001-2009) in the south-east of Australia (Fowler
113 et al., 2016; King et al., 2020; Kirono et al., 2017; Potter et al., 2010; Saft et al., 2016, 2015; Van Dijk et al.,
114 2013). As such, a holistic understanding of concurrent changes in hydroclimatic variables across Australia
115 does not currently exist. Here, we use a high-resolution continental water balance model to study trends
116 in simulated streamflow across the Australian continent, along with drought and high flow (flood) indices,
117 according to their key drivers: rainfall, evapotranspiration, and soil moisture. We test the model's ability
118 to reproduce hydrological trends then use the model as a tool to quantify historical trends across the
119 water balance.

120 **2 Methodology**

121 The approach used for this study is as follows:

- 122 1. The Australian Water Resource Assessment -Landscape model (AWRA-L) model is assessed in terms
123 of simulated runoff reproduction of streamflow trends at a set of high-quality catchments; with
124 catchment trend assessment grouped according to climatologically similar regions;

- 125 2. Spatial trends in simulated runoff (aggregated to streamflow) are compared to trends in rainfall,
126 potential evaporation (PET), actual evapotranspiration (AET), and soil moisture.
- 127 3. Trends in catchment scale runoff extremes (drought and flood indices) are compared to trends in
128 related hydrologic and climate indices (i.e. mean rainfall and soil moisture trends, and trends in
129 extreme rainfall).

130 **2.1 AWRA-L Model**

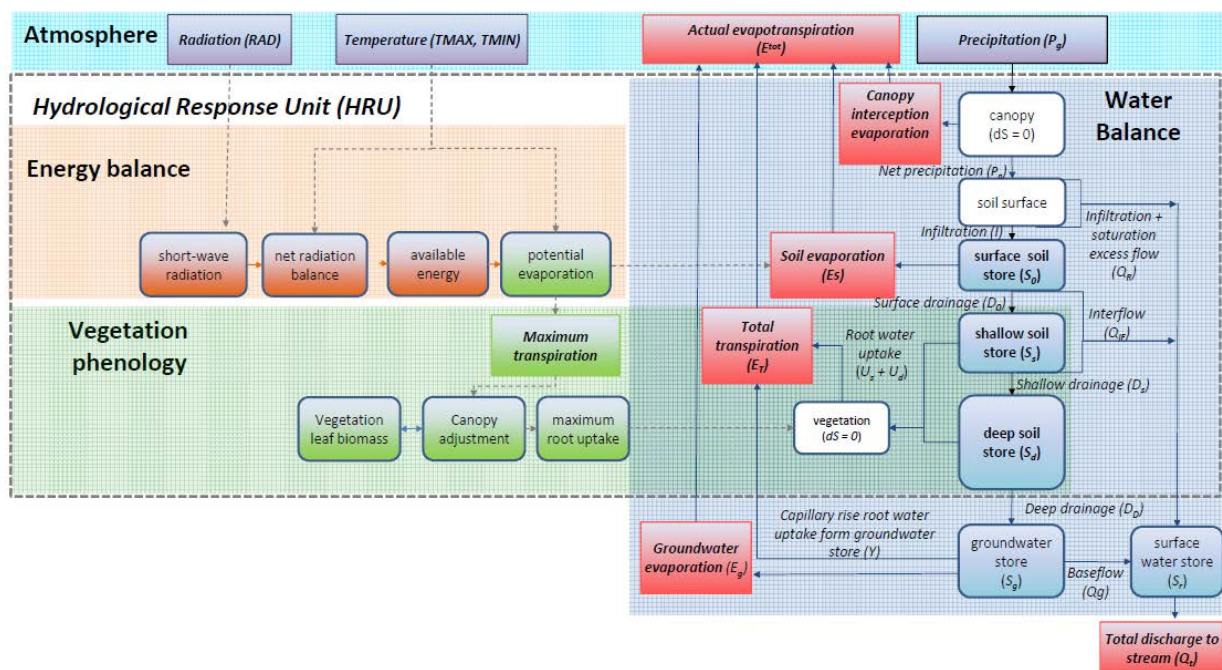
131 AWRA-L is a daily, gridded, one-dimensional, semi-distributed continental-scale landscape water balance
132 model developed by the CSIRO and the Australian Bureau of Meteorology (BOM) (Frost et al., 2018; Van
133 Dijk, 2010; Viney et al., 2015) for water resource assessment and monitoring. It is currently run
134 operationally to provide near real-time hydrological data at a resolution of 0.05° x 0.05° (approximately
135 5km x 5km) from 1911 to the present across Australia (see www.bom.gov.au/water/landscape). Figure 1
136 presents the climate inputs, hydrological outputs, and simulated processes in AWRA-L.

137 The model forcing inputs are daily solar radiation, minimum and maximum temperature, 2m wind speed,
138 and precipitation. Other static inputs describe the spatial variability of soil and geological properties and
139 land use. In its operational use, AWRA-L uses daily precipitation and maximum and minimum
140 temperatures obtained from the Australian Water Availability Product (AWAP) (Jones et al., 2009),
141 remotely-sensed solar radiation (Grant et al., 2008), and an interpolated field of station-based
142 observations of wind speed (McVicar et al., 2008). Daily varying climatologies of solar radiation and wind
143 speed are used prior to 1990 and 1975, respectively, prior to the relevant observational datasets
144 becoming available.

145 The key hydrologic processes modelled include: 1) partitioning of rainfall between interception and water
146 contributing to the water balance; 2) infiltration or saturation excess surface runoff dependent on
147 groundwater saturation; 3) interflow, drainage, and evaporation from the soil layers; and 4) baseflow and
148 evapotranspiration from the groundwater store. Potential evaporation is modelled using the Penman
149 equation (Penman, 1948), which uses wind and temperature as inputs, along with solar radiation to
150 calculate the terrestrial energy balance following Donohue et al. (2010). The soil is modelled in three layers
151 (0-0.1m, 0.1-1m, and 1-6m depth) with differing model parameters between layers. Shallow rooted
152 vegetation has access to soil moisture in the upper two layers while deep rooted vegetation also has
153 access to the bottom most layer. Key output fluxes are runoff, actual evapotranspiration, and soil moisture
154 for the three soil layers and deep drainage to the groundwater store. Similar to other semi-distributed

155 models, the total runoff from a grid cell is a summation of the surface and subsurface runoff fluxes.
 156 AWRA-L contains 49 parameters, of which 28 are fixed according to previous parameter sensitivity
 157 experiments and prior knowledge, and 21 are optimised to maximise an objective function that considers
 158 performance against observed streamflow (covering the period 1981-2011), remotely sensed
 159 evapotranspiration, and remotely sensed surface soil moisture at a set of 295 unimpaired catchments
 160 (Zhang et al., 2011). The reader is referred to Viney et al. (2015) and Frost et al. (2018) for further details.

161



162

163 **Figure 1.** AWRA-L conceptual structure. Purple: climate inputs; Blue rounded boxes: water stores; Red
 164 boxes: water flux outputs; Brown: energy balance; Green rounded boxes: vegetation processes. The
 165 dotted line indicates processes modelled in each grid cell (Frost et al., 2018).

166 Verification is undertaken firstly to the calibration data at independent sites (streamflow and remotely
 167 sensed estimates of catchment average soil moisture and evapotranspiration over a separate set of 291
 168 unimpaired catchments); along with in-situ measurements of soil moisture, flux tower estimates of
 169 evapotranspiration, and estimates of groundwater recharge nationally; see Frost and Wright (2018).
 170 AWRA-L performs well compared to other available continental scale models for streamflow
 171 (predominantly due to streamflow data being used in calibration), and similarly to locally calibrated
 172 nearest-neighbour regionalised conceptual rainfall runoff models, giving confidence that AWRA-L can be

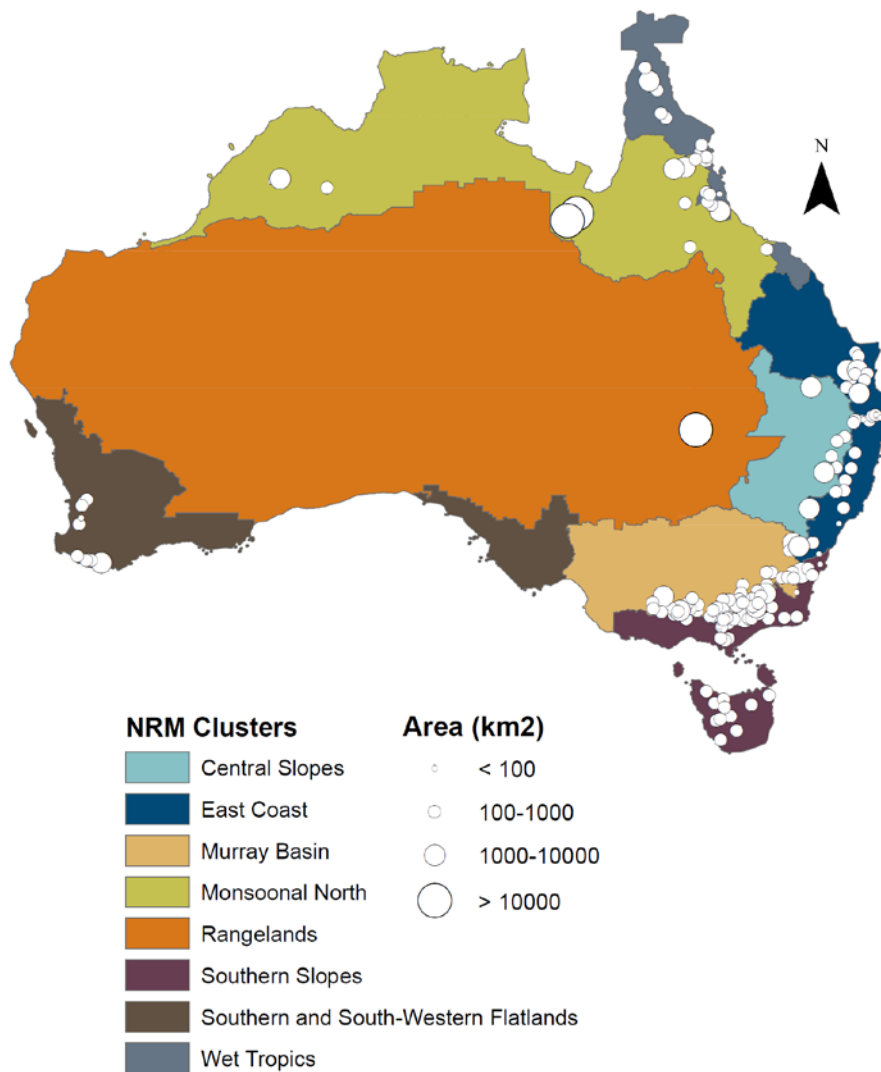
173 considered a fit-for-purpose continental scale hydrological model for water resource and agricultural
174 applications. Similarly, AWRA-L compares well to continental scale models when assessed against in-situ
175 root-zone (0-90cm) soil moisture observations, and shows comparable (if not better) correlation to in-situ
176 and remotely sensed data (Holgate et al., 2016), with soil moisture variability representative of catchment
177 dynamics (Peterson et al., 2020). AWRA-L shows comparable performance over other continental scale
178 models for evapotranspiration but currently shows slightly poorer performance according to annual
179 correlation of deep drainage (Frost and Wright, 2018).

180 As a result of this performance across the water balance, AWRA-L forms an integral part of the Australian
181 Bureau of Meteorology's national water accounting, water monitoring (Elmahdi et al., 2016; Hafeez et al.,
182 2015), and estimation of antecedent conditions for event-based flood forecasting. It has been used in
183 retrospective studies for national flood design guidelines (Ball et al., 2019), to understand the impact of
184 changes in soil moisture on flood magnitude (Wasko and Nathan, 2019a) and flood timing (Wasko et al.,
185 2020), and for the identification of flash drought using the evaporative stress index (Nguyen et al., 2019).

186 **2.2 Analysis**

187 **2.2.1 Regional grouping**

188 Broadly, Australia's climate varies from tropical in the north to temperate in the south with an arid climate
189 inland. The north generally receives monsoon-driven rainfall in warmer months (November to April) with
190 little to no rainfall in the colder months (May to October), with rainfall becoming more seasonally uniform
191 moving south. The exception is the south-east which experiences a dry austral summer and wet colder
192 months. A small mountain range that runs along the east coast of Australia demarcates regions with less
193 rainfall inland and more rainfall towards the coast. Recognising these differences in climate, we
194 (regionally) aggregate and discuss results based on clusters of Natural Resource Management (NRM)
195 regions. For consistency with the other work in Australia (CSIRO and Bureau of Meteorology, 2015) the
196 NRM regions are defined by catchments and bioregions of similar climatic conditions (Figure 2). We note
197 that the Murray Basin region presented here forms the lower part of the larger Murray Darling Basin, one
198 of the most significant agricultural regions in Australia.



199

200 **Figure 2.** Hydrologic reference stations underlain by Natural Resource Management (NRM) regions.

201 **2.2.2 Evaluation of simulated streamflow trends**

202 Although AWRA-L has been extensively validated, the ability of AWRA-L to capture observed hydrological
 203 trends has not been previously tested. Observed (historical) trends in potential evapotranspiration (PET),
 204 actual evapotranspiration (AET), and soil moisture (SM) are traditionally inconsistent and data source
 205 dependent (see Section 1.2). For this reason, and because streamflow is an integration of the above fluxes
 206 and stores, we focus on evaluating trends in catchment-aggregated AWRA-L runoff representing
 207 streamflow. It is reasonable to assume that the unrouted, simulated runoff can be aggregated to

208 represent streamflow in smaller catchments where streambed losses are smaller and routing impacts less.
 209 Simulated trends in catchment-aggregated AWRA-L runoff are evaluated against trends in observed
 210 monthly streamflow at a set of high quality observational hydrologic reference stations (Zhang et al.,
 211 2016). These stations represent relatively unaltered catchments (low urbanisation, irrigation, forestry
 212 effects). In total 160 stations of varying length are used. Most stations have recordings beginning in the
 213 1970s with the longest length of record 37 years, shortest 19 years, and a median record length of 35
 214 years. Station locations are presented in Figure 2 with the reader referred to Zhang et al. (2016) for further
 215 details of this data set.

216 **2.2.3 Trends in simulated hydroclimatic variables and indicators of flood and drought**

217 Trends in observed streamflow, rainfall (AWAP), and simulated PET, AET, soil moisture, and runoff are
 218 calculated as the slope of a linear regression of the seasonal or annual means of the respective variable.
 219 Results focus on the period 1960-2017, coinciding with the increase in temperature identified post 1960
 220 due to anthropogenic climate change (Fawcett et al., 2012). Here, we analyse root-zone soil moisture (0-
 221 100cm soil depth), as it is most correlated with catchment flood response (Hill et al., 2016; Hill and
 222 Thomson, 2019) modulating streamflow at various levels of event severity (Wasko et al., 2020; Wasko and
 223 Nathan, 2019a).

224 Trends in high (flood) and low (drought) flow indicators were also examined and compared to trends in
 225 rainfall and evapotranspiration and runoff. Here we use the 90th percentile (q90) of annual daily flow and
 226 5-day (5day) annual maxima for high flows/floods. The standardised runoff index (SRI) is used to
 227 characterise drought (Shukla and Wood, 2008). The SRI is defined by fitting a probability distribution to
 228 the runoff time-series (in this case either gamma, log-normal, or normal based on the best fit) and
 229 converting the fitted cumulative distribution to a standard normal deviate. Here, the SRI-12 (based on a
 230 12-month calendar year aggregate) is used. The definitions, or classifications, of drought (McKee et al.,
 231 1993) according to SRI-12 are presented in Table 1. As an indicator of drought extent, for each NRM region
 232 the trend in the proportion of grid cells experiencing drought, as defined by the SRI-12 categories
 233 presented in Table 1, is also calculated.

234 Table 1. Classification of drought category using the standardised runoff index (SRI)

SRI Value	Drought Category	Time in category (%)
-1.00 to -1.49	Moderate	9.2
-1.50 to -1.99	Severe	4.4

235

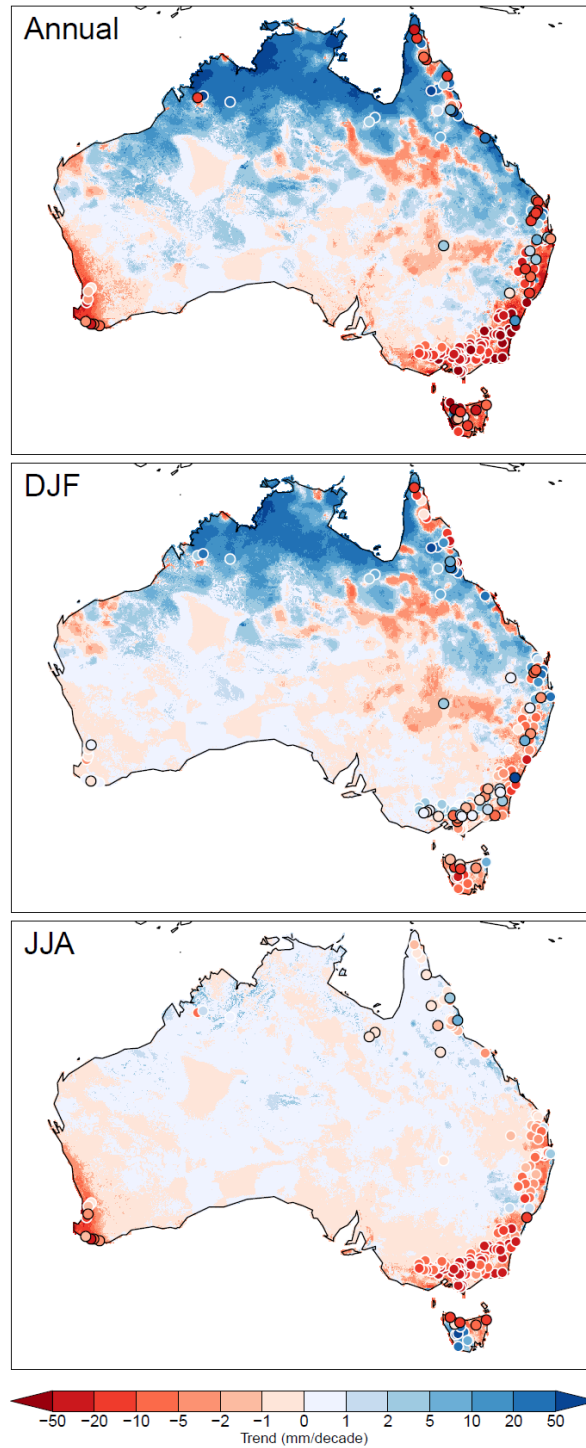
236 3. Results

237 The results are presented as follows: first AWRA-L streamflow trends are evaluated against observed
238 trends. Next the continental scale trends in seasonal and annual means of AWAP (observed) rainfall, and
239 simulated PET, AET, soil moisture, and runoff are presented. Trends in indicators of flood/drought are also
240 evaluated. Finally, results are regionally aggregated across NRM regions. Trends are presented as scatter
241 plots between variables to understand how trends interact at catchment scale, whether there are
242 differences in the interaction regionally, and how these interactions compare to interactions at the
243 continental scale.

244 3.1 Catchment streamflow trend verification

245 The observed streamflow trend underlain by simulated AWRA-L runoff for 1960 to 2017 is presented in
246 Figure 3. Circles with white outline indicate that the direction of observed and modelled trends matches,
247 whereas black circles indicate the direction of trends does not match. Although AWRA-L runoff on a grid
248 cell basis is not directly comparable to streamflow which is a catchment outflow, regional coherence of
249 observed and modelled trends is promising. On an annual basis AWRA-L runoff and observed streamflow
250 in the south-west and south-east of the continent show strong decreasing trends. In the central north of
251 the continent there are increasing trends both in observations and simulations, but simulations of the
252 north-east coast display some divergence from observations. There appears to be localised decreases in
253 observed streamflow along the north-east coast and at the very far south-west tip of the continent which
254 are not captured by AWRA-L.

255 In the north of the continent, rainfall and streamflow is warm month dominant (DJF). The local variations
256 in streamflow appear to be better captured in the north-east of the country which is promising as these
257 are the months of largest trend. In the south of the country, where the trends are now small, there is
258 localised increasing runoff modelled matching the observed trends for some locations. In the south of the
259 continent, rainfall and streamflow is winter (JJA) dominant, and the strong decreasing trends are
260 simulated well. For Tasmania, the island off the south-east coast of Australia, the strong gradient in
261 observed trends between the east and west coast is captured (although being slightly displaced). For the
262 northern winter (JJA) there is little trend and the modelled runoff likewise shows little trend. The general
263 small but decreasing trend for winter runoff along the east coast moving north is captured.

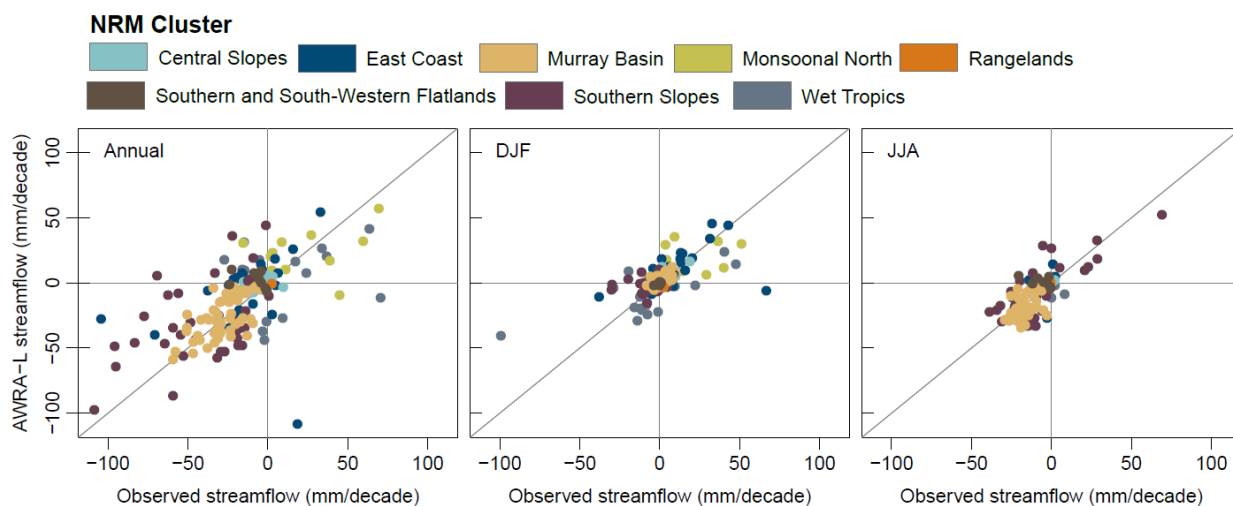


264

265 **Figure 3.** Observed trends in streamflow for 160 HRS catchments across Australia underlain by
 266 simulated AWRA-L runoff. Results are presented annually, for the austral summer months (DJF), and the
 267 austral winter (JJA). White circles indicate that the direction of the modelled trend and observed trend

268 match. Black circles indicate that the direction of the modelled trend and observed trend does not
269 match. For consistency, the runoff trend is for 1960 to 2017.

270 Seasonal and annual linear trends in simulated AWRA-L aggregated runoff (streamflow) are compared
271 with observed streamflow on a catchment by catchment basis in Figure 4. For each catchment the
272 modelled streamflow is a summation of the runoff for all the grid cells within the catchment (Section
273 2.2.2). Performance is compared on the basis of the NRM regions presented in Figure 2, noting that we
274 assume the catchments are representative of the climatic conditions in that region. The coefficient of
275 determination (r^2) and the hit rates annually and for each season are presented in Table 2. The hit rate
276 corresponds to when the direction is correctly modelled, that is, the observed and simulated trends are
277 both in the top-right (positive-positive) or bottom-left (negative-negative) quadrants in Figure 4.
278 Simulated annual flow direction trend matches that observed at 122 of the 160 (76%) sites with an overall
279 coefficient of determination of 0.38 (Table 2). In particular, the direction of simulated trend matches the
280 observed for all sites in the Murray Basin, and good correspondence is found for the Southern Slopes with
281 76% of the sites matching in simulated and modeled trend direction. For the Monsoonal North, despite
282 82% sites matching in trend direction, the coefficient of determination is low due to a large scatter in the
283 observed and modelled trends (Figure 4).



284
285 **Figure 4.** Scatter plot of simulated and observed trends in seasonal and annual runoff for 160 HRS
286 catchments across Australia. Catchment locations are shown in Figure 3. Results are presented annually,
287 for the austral summer months (DJF), and the austral winter (JJA). The hit rate and coefficient
288 determination for each of the regions is presented in Table 1.

289 **Table 2.** The number of sites where the modelled catchment streamflow trends matches the observed
 290 catchment streamflow trend (hit rate) and the coefficient of determination (r^2) between the modelled
 291 and observed trends. Results are presented annually, for the austral summer months (DJF), and the
 292 austral winter (JJA).

NRM Region	Hit rate (%)	r^2
Annual		
Wet Tropics	10 out of 17 (59%)	0.05
Monsoonal North	9 out of 11 (82%)	0.07
East Coast	14 out of 26 (54%)	0.08
Central Slopes	6 out 10 (60%)	0.30
Southern Slopes	25 out of 33 (76%)	0.26
Murray Basin	53 out of 53 (100%)	0.44
Rangelands	0 out of 1 (0%)	-
Southern and South-Western Flatlands	5 out of 9 (56%)	0.21
Overall	122 out of 160 (76%)	0.38
DJF		
Wet Tropics	14 out of 17 (82%)	0.54
Monsoonal North	11 out of 11 (100%)	0.06
East Coast	20 out of 26 (77%)	0.33
Central Slopes	8 out 10 (80%)	0.67
Southern Slopes	21 out of 33 (64%)	0.03
Murray Basin	41 out of 53 (77%)	0.34
Rangelands	0 out of 1 (0%)	-
Southern and South-Western Flatlands	7 out of 9 (78%)	0.37
Overall	122 out of 160 (76%)	0.43
JJA		
Wet Tropics	14 out of 17 (82%)	0.24
Monsoonal North	6 out of 11 (55%)	0.43
East Coast	25 out of 26 (96%)	0.13
Central Slopes	10 out 10 (100%)	0.25
Southern Slopes	28 out of 33 (85%)	0.59

Murray Basin	53 out of 53 (100%)	0.38
Rangelands	1 out of 1 (100%)	-
Southern and South-Western Flatlands	4 out of 9 (44%)	0.34
Overall	141 out 160 (88%)	0.55

293

294 The overall annual results can mask the results for the dominant streamflow season (Table 1). For summer
 295 (DJF), the r^2 between trends is 0.06 and 0.54 for the Monsoonal North and Wet Tropics respectively,
 296 however 11 of 11 sites (100%) in the Monsoonal North, and 14 out of 17 sites (82%) in the Wet Tropics
 297 model the observed trend direction suggesting better correspondence in the summer (wet) months than
 298 when streamflow is aggregated for the year. Good correspondence is observed for the East Coast and
 299 Central Slopes in the winter (JJA) where AWRA-L simulates the observed trend direction at 35 of 36 sites.
 300 Similarly, for the Murray Basin, all sites have the same modelled trend direction in the winter (the
 301 dominant streamflow season). In comparison, in the summer, where there is the least flow, 41 out of 53
 302 Murray Basin sites correctly model the observed trend direction (77%). Streamflow is winter dominant in
 303 the Southern Slopes. Here 28 out of 33 (85%) sites model the correct trend direction with an r^2 of 0.59. At
 304 the catchment scale, the Southern and South-Western Flatlands exhibit the lowest skill, with the correct
 305 direction modelled at only 4 out of the 9 sites in the winter, possibly due to very differing local geology.

306 Overall, the modelled and observed trends compare well (Figure 3). At a majority of observational sites,
 307 streamflow trends are reproduced by AWRA-L, giving confidence in using simulated water balance
 308 variables to support our interpretations of the observed trends. The direction of the streamflow trend is
 309 well reproduced, particularly for the dominant streamflow season, but the magnitude of the trend is not
 310 necessarily represented well in parts of the tropics. Best correspondence is found in the south-east of the
 311 country (Murray Basin and Southern Slopes regions). Evaluation was also performed for the 90th percentile
 312 of streamflow with results largely similar to those presented here.

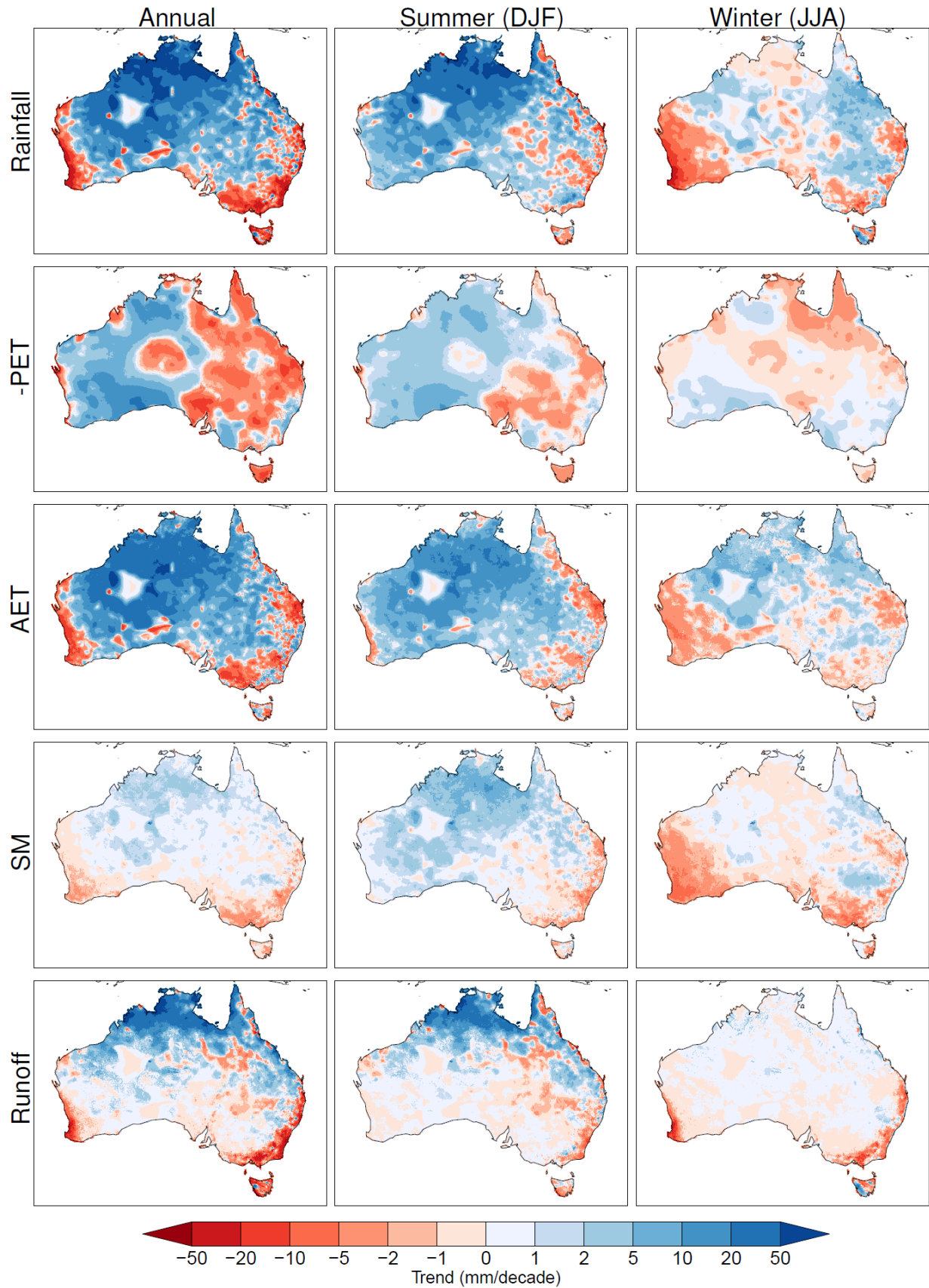
313 **3.2 Continental scale trends in hydroclimatological variables**

314 Having established the verification of AWRA-L, trends in the (simulated) hydrologic variables are now
 315 evaluated. Figure 5 presents the trend in observed rainfall (derived from the gridded interpolated climate
 316 observations) as well as simulated potential and actual evapotranspiration, soil moisture, and runoff for
 317 the period 1960 to 2017. Two key points are noticeable for the annual rainfall trends: a positive trend for
 318 the summer dominated tropical monsoonal north, and a negative trend for the autumn/winter frontal

319 system dominated south. Tropical rainfall in northern Australia is summer (DJF) dominant and has been
320 increasing over the last half a century. With little rain occurring in the winter (JJA) in these areas, the trend
321 observed in winter is negligible, and the annual trend is dominated by changes in summer rainfall. In
322 general summer rainfall has been increasing across Australia, but this trend is less clear in the east, for
323 example isolated coastal areas on the east coast exhibit decreases in summer rainfall. The annual trend
324 in rainfall for the south-west is strongly influenced by decreasing winter rainfall. In the south-east of
325 Australia, a similar trend is observed – there is a decline in winter rainfall (though the largest observed
326 decrease is for autumn rainfall) resulting in decreased mean annual rainfalls. Although trends are
327 presented for all of Australia, we note that the rainfall gauging network in the arid center of Australia is
328 limited, with high uncertainty in these areas. Hence the interpretation of results is limited to coastal, more
329 populous, and streamflow producing regions.

330 Notionally, trends in PET could be expected to be proportional to changes in temperature or inversely
331 proportional to rainfall due to increased cloud cover. But as discussed in the introduction there are many
332 confounding factors and interdependencies affecting PET trends. Figure 5 presents, for the period 1960-
333 2017, decreases in PET across the western half of Australia in summer and increases across the eastern
334 half of Australia. There is a slight decrease in PET for the winter months in southern Australia and an
335 increase in PET in northern Australia, but overall, the annual trend from east to west appears dominated
336 by the trend in summer PET. There is little evidence for a spatial correlation of these trends with changes
337 in rainfall or the increase in temperature observed across Australia over the past half a century. However,
338 it should be noted that the driving radiation and wind variables for the PET simulated here are based on
339 climatologies pre 1990 and 1975 respectively.

340



342 **Figure 5.** Linear trend in rainfall, potential evapotranspiration (PET), actual evapotranspiration (AET), soil
343 moisture (SM), and runoff from 1960 to 2017. Results are presented annually, for the austral summer
344 months (DJF), and the austral winter (JJA). Note that we plot -PET here for ease of visual colour
345 comparison.

346 The modelled AET displays very similar trends to the rainfall, confirming that, with the exception of some
347 coastal areas (primarily the south-east coast), evapotranspiration across most of Australia is water (and not
348 energy) limited. In the summer months there is an increase in evapotranspiration across the tropical
349 north, with decreases elsewhere. In the winter, there is a strong spatially coherent signal in the
350 evapotranspiration, with decreases in the south-west, corresponding to decreases in availability of
351 moisture due to declines in rainfall. The result is an annual trend in AET and rainfall of similar magnitude,
352 between 10-50 mm/decade in the central northern tropics with decreases of a similar magnitude in the
353 south-west of Australia.

354 For consistency, the units of the soil moisture trends are the same. As soil moisture trends are presented
355 for the top 1m of soil, the magnitude of the trend may be less, despite its large modulating effect on flood
356 response (Wasko and Nathan, 2019a). Soil moisture tends towards wetting in the summer in the north
357 and west of Australia, with a drying trend only present in the south-west and south-east. In the winter
358 there is almost universal drying across the south of Australia resulting in an annual trend similar to rainfall
359 and AET trends. There are increases in soil moisture in the north of Australia and decreases in the south,
360 consistent with trends in rainfall and water availability. However, arguably, the changes in soil moisture
361 are more spatially consistent, an indicator of the longer residence time of water in the soil. For example,
362 the drying trend across the east coast in soil moisture is much more extensive compared to the AET trend
363 comprised of a mixture of increasing and decreasing trends.

364 The observed changes (trends) in rainfall and soil moisture translate to large changes in runoff across
365 Australia. In the central tropics there is an increase in runoff in the summer of over 50mm/decade, while
366 along the south-east coast there is a small drying trend of approximately 5-10mm/decade. In winter, the
367 south-east and south-west coasts exhibit large decreasing trends in the order of 20mm/decade. In the
368 north, winter is the dry season and there are no significant trends. The high spatial resolution of AWRA-L
369 results in regional differences being modelled. For example, for Tasmania, the island off the south-east
370 coast of Australia, a decreasing trend is modelled on the east-coast, and increasing trend on the west-
371 coast, commensurate with the orographic divide that runs north-south. Similarly, across the south-east
372 coast of Australia greater decreasing trends in runoff are observed on the coastal side of the dividing

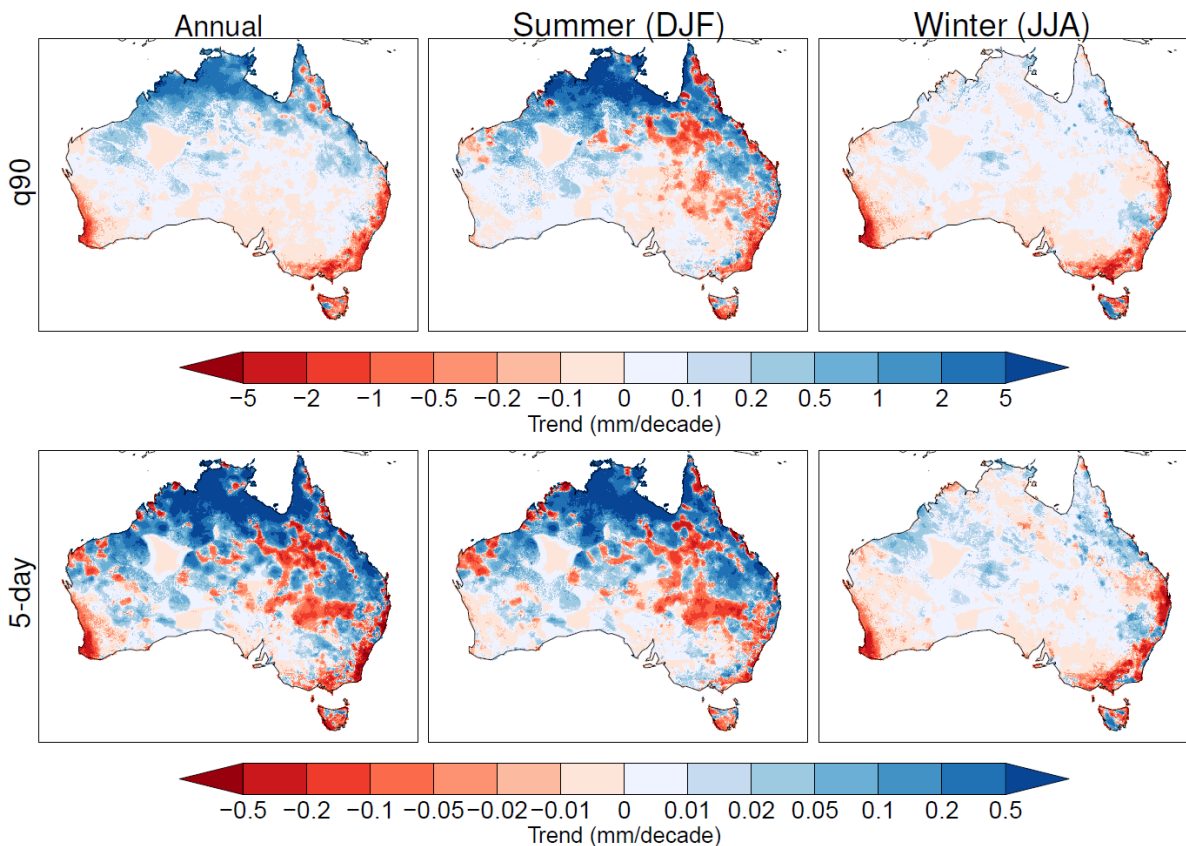
373 mountain range that runs along the east coast. There is little trend in runoff elsewhere, with most trends
374 in runoff across Australia contained to the coastal areas of higher rainfall.

375 **3.3 Trends in high flow indices**

376 The continental pattern across Australia for the 90th percentile (q90) of daily runoff (on an annual basis)
377 and the 5-day maxima from 1960 to 2017 are presented in Figure 6. The trends in the 90th percentile
378 runoff (top row) reflect the mean runoff trends presented in Figure 5, suggesting a uniform directional
379 shift in the flow distribution, similar to global studies (Gudmundsson et al., 2019). There are decreases for
380 q90 in the summer months (DJF) for the tropical north and parts of the south-east coast. Although rainfall
381 and runoff are summer dominant along the north-east coast the trends are mixed and there is little trend
382 elsewhere due to low summer rainfall. For winter months (JJA) there are large reductions in q90 across
383 the southern coast of Australia with little trend elsewhere, coinciding with the lack of rainfall and runoff
384 across the northern parts of Australia in the winter. On a continental scale, the annual trend reflects the
385 summation of the seasonal patterns.

386 The 5-day annual maxima (bottom row) is more extreme than the 90th percentile and hence the trends
387 exhibit greater variability than the trends for q90. Compared to the trend in q90 there are now more
388 increases in the extreme runoff on the south-east coast reflecting how the more extreme the rainfall, the
389 more likely we are to see increases, particular in the winter months when rainfall seasonality is dominant
390 across south-west Australia. The annual trends form a different composite of the results presented for
391 the 90th percentile. In the summer months the trend in the 5-day annual maxima remains similar to q90,
392 but for winter the trends exhibit more variability with more wetting trends exhibited on the south-east
393 coast of Australia. The 5-day maxima for eastern inland areas of Australia is influenced more by trends in
394 the summer (and not winter) months while the northern part of Australia is influenced by the summer
395 trends.

396 Despite predicted increases in extreme rainfall across Australia (Guerreiro et al., 2018) there remain large
397 parts of the country with observed decreasing trends in q90 and the 5-day annual runoff maxima. This
398 indicates that events at this level of severity are controlled by other processes than simply changes in
399 extreme rainfall, for example changing rainfall persistence characteristics and changing soil moisture (e.g.
400 Wasko and Nathan, 2019a). The mean runoff drying trend (Figure 5) is strongest in the south-west of
401 Australia and this continues to be reflected with the q90 and 5-day annual maxima decreasing uniformly
402 on the south-west coast (Figure 6).



404

405 **Figure 6.** Linear trend in 90th percentile (q90) and annual maxima (5-day) for runoff from 1960 to 2017.

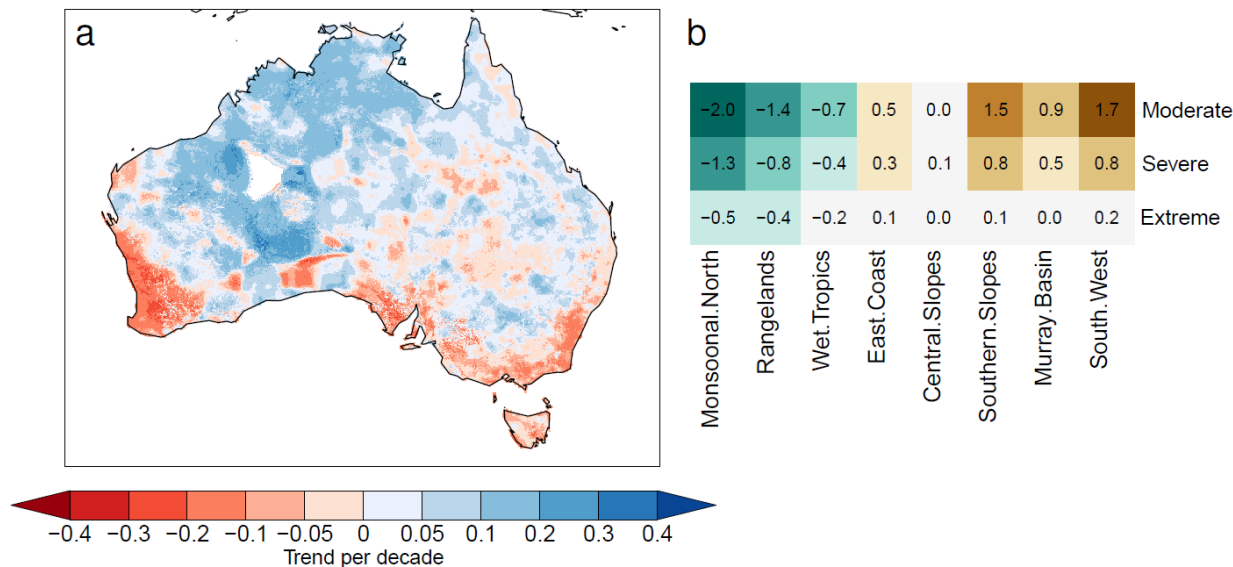
406 Results are presented annually, for the austral summer months (DJF), and the austral winter (JJA).

407 3.4 Trends in low flow indices

408 Drought, or low flow, trends are quantified using the SRI-12 (Figure 7). SRI drought is relative to the
 409 variability at the individual pixel, hence by definition large parts of Australia will experience drought
 410 although they may not necessarily experience small mean rainfall. This is a limitation of using the SRI to
 411 characterise drought, particularly in regions of low flow (such as the arid interior of Australia).
 412 Correspondingly, we focus our analysis on the northern and coastal regions.

413 The SRI-12 is trending towards drier conditions around and inland of the southern half of the continent
 414 (Figure 7a) consistent with decreased runoff/streamflow (Figure 5). Across the Southern Slopes and
 415 Southern and South-Western Flatlands, there is a consistent negative trend in the SRI-12 indicating a shift
 416 to drier conditions and more frequent drought conditions. There is no single indicator of drought (Kiem
 417 et al., 2016), hence these results should be interpreted with respect to the trends in hydroclimatic

418 variables presented in Figure 5. What is starkly different from the previous results is that not just the
 419 south-west and south-east of Australia are trending towards drier conditions but most of southern
 420 Australia is experiencing drier conditions. This points to how multiple indicators of drying conditions, in
 421 the context of internal variability, need to be considered (e.g. Nathan et al., 2019).



422
 423 **Figure 7.** Trend in annual SRI from 1960 to 2017 (a) continental trends (b) change in the proportion
 424 (%/decade) of grid cells experiencing drought based on annual SRI (Table 1). Increases are shaded in
 425 brown and decreases are shaded in green.

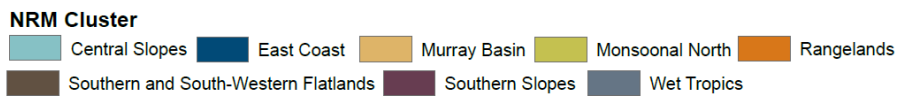
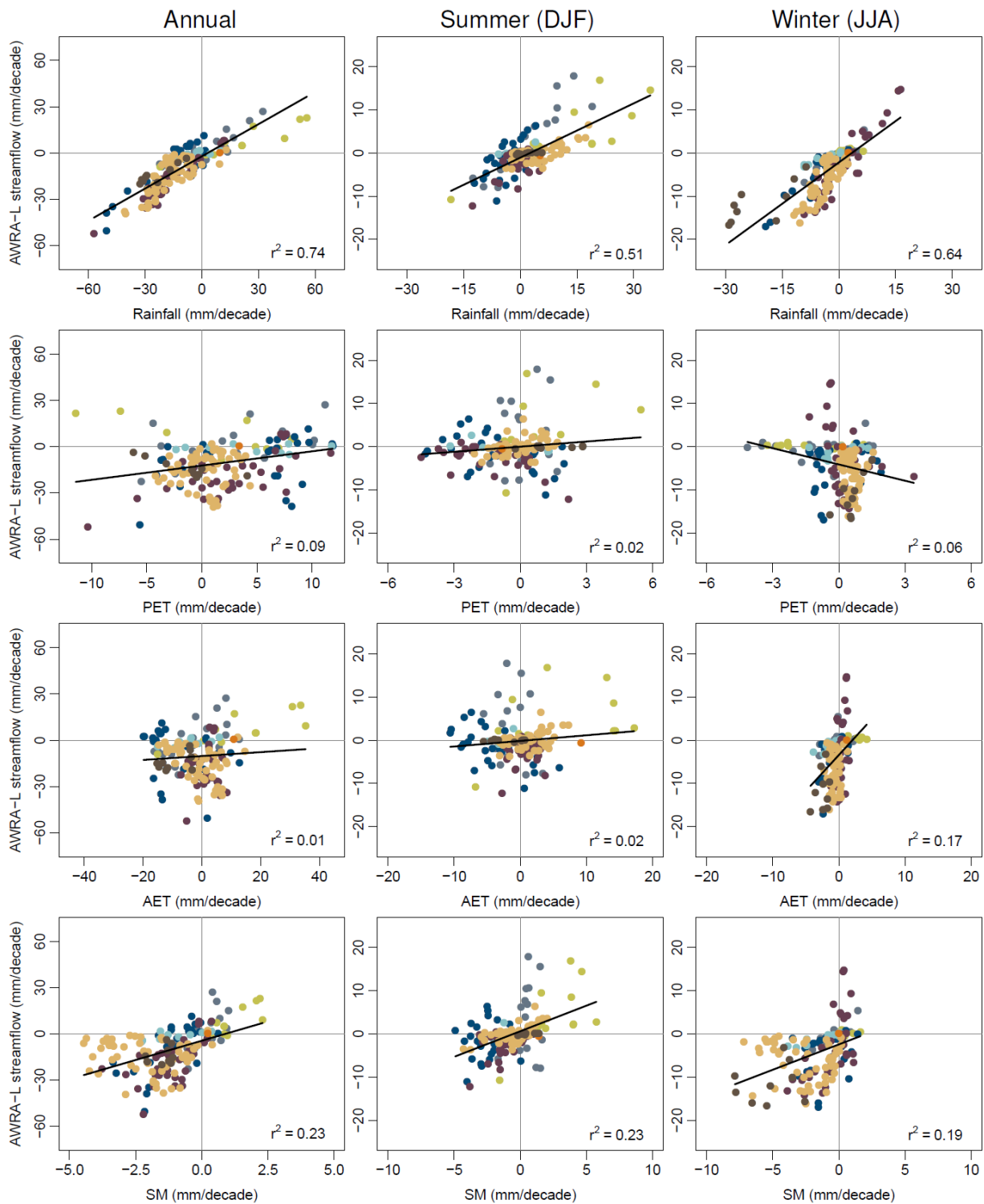
426 As an indicator of changes in drought extent, the change in the percentage of grid cells experiencing
 427 drought in each year in each of the NRM regions was calculated (Figure 7b). A 1% per decade
 428 represents an increase in the percentage of grid cells in an NRM observing drought (e.g. from 25% to 26%).
 429 The decreasing number of cells in the Monsoonal North, Rangelands, and Wet Tropics suggests a smaller
 430 extent of drought with climate change, consistent with the increases in mean rainfall presented in
 431 Figure 5. But we note that there were localised regions trending to lower SRI-12 (i.e. drought) in the Wet
 432 Tropics (Figure 7a). The greatest increase in the number of cells experiencing drought occurs in the
 433 Southern Slopes, Murray Basin and Southern and South-Western Flatlands. The large increasing extent of
 434 drought and decreasing mean annual rainfall in the Murray Basin is concerning, as this is a significant
 435 agricultural region for Australia.

436
 437

438 **3.5 Catchment scale interaction of hydroclimatological variables**

439 Section 3.2 presented a continental scale analysis of changes in the drivers of streamflow across Australia.
440 However, trends and interactions of hydroclimatological variables at the catchment scale are likely to
441 differ from those at the continental scale (Saft et al., 2015; Whitfield, 2012). Focusing on streamflow,
442 Figure 8 presents simulated streamflow trends against trends in observed rainfall and simulated PET, AET,
443 and soil moisture. We note that simulated streamflow is a summation of the AWRA-L runoff (Section
444 2.2.2).

445 There is a strong correspondence between rainfall and simulated streamflow trends both seasonally and
446 annually, with an r^2 of 0.74 at the annual timescale. It is very evident that the strongest positive trends in
447 streamflow and rainfall occur in the Wet Tropics and Monsoonal North, and largely in the wet season
448 (austral summer) months (DJF). Conversely the decrease in streamflow in the Southern and South-
449 Western Flatlands is largely a result of winter (JJA) rainfall declines. This confirms the findings presented
450 in the gridded results in Figure 5. But it is now also clear, which was not evident previously, that the
451 Southern Slopes and Murray Basin regions, although adjacent, have markedly different behavior as a
452 result of an orographic divide. Although mean annual rainfall and streamflow are reducing across both
453 regions at the annual scale, summer rainfall and streamflow are increasing in the Murray Basin. In the
454 winter the Southern Slopes have increasing rainfall and streamflow.



457 **Figure 8.** Simulated streamflow trend per decade for 160 catchments across Australia from 1960 to 2017
458 against trend in potential evapotranspiration (PET), actual evapotranspiration (AET), and soil moisture
459 (SM). Results are presented annually, for the austral summer months (DJF), and the austral winter (JJA).
460 Catchment locations are shown in Figure 2. A line of best fit is presented in black with the coefficient of
461 determination (r^2) for each pair of variables. Coefficients of determination for individual NRM regions
462 are presented in Table S1.

463 Similar to the continental trends, there is little correspondence between PET and runoff at catchment
464 scale. This is because, firstly, the trend in PET is only realised as a trend in either AET, soil moisture, or
465 runoff if there is sufficient moisture available (and it will appear in AET and soil moisture before runoff
466 which is an integration of the above fluxes). Secondly, the trends in PET are small compared to rainfall.
467 Despite strong continental coherence in AET and runoff trends (Figure 5), regional scale trends between
468 AET and runoff generally have very low coefficients of determination (Table S1) with the exception of the
469 Wet Tropics, Monsoonal North and Southern and South-Western Flatlands. This suggest, for these
470 regions, greater runoff is correlated with greater evapotranspiration probably due to greater water
471 availability through greater precipitation. The Wet Tropics, Monsoonal North, and Southern and South-
472 Western Flatlands are wetter coastal regions and therefore are possibly not moisture limited but energy
473 limited. However, regions like the Southern Slopes and East Coast are also coastal, and do not have a
474 strong relationship between AET and runoff (annually), implying, not all coastal regions are energy limited.
475 It does not appear that AET is driving changes in streamflow, as the strong positive relationship between
476 AET and runoff for the Southern and South-Western Flatlands is counter to the fact that runoff is
477 decreasing in this region reducing water availability.

478 Soil moisture is more strongly linked to streamflow (r^2 of 0.23 annually) than AET (r^2 of 0.01) or PET (r^2 of
479 0.09), suggesting wet soils are contributing to runoff and vice versa. The strength of these relationships
480 does not necessarily correspond to the seasonality of streamflow. For example, there is a strong
481 relationship in the summer months in the Murray Basin between runoff and soil moisture (r^2 of 0.40) and
482 similarly for the Southern and South-Western Flatlands (r^2 of 0.49) but these are the months of the lowest
483 streamflow. For winter streamflow, the relationship between soil moisture and streamflow is more
484 random, suggesting that streamflow depends more on rainfall in wetter months whereas in drier months
485 the relationship between streamflow and rainfall is modulated by soil moisture.

486 The lack of relationships in trend between soil moisture and runoff in the winter months for the Murray
487 Basin and Southern and South-Western Flatlands is reflected in the annual relationship where little

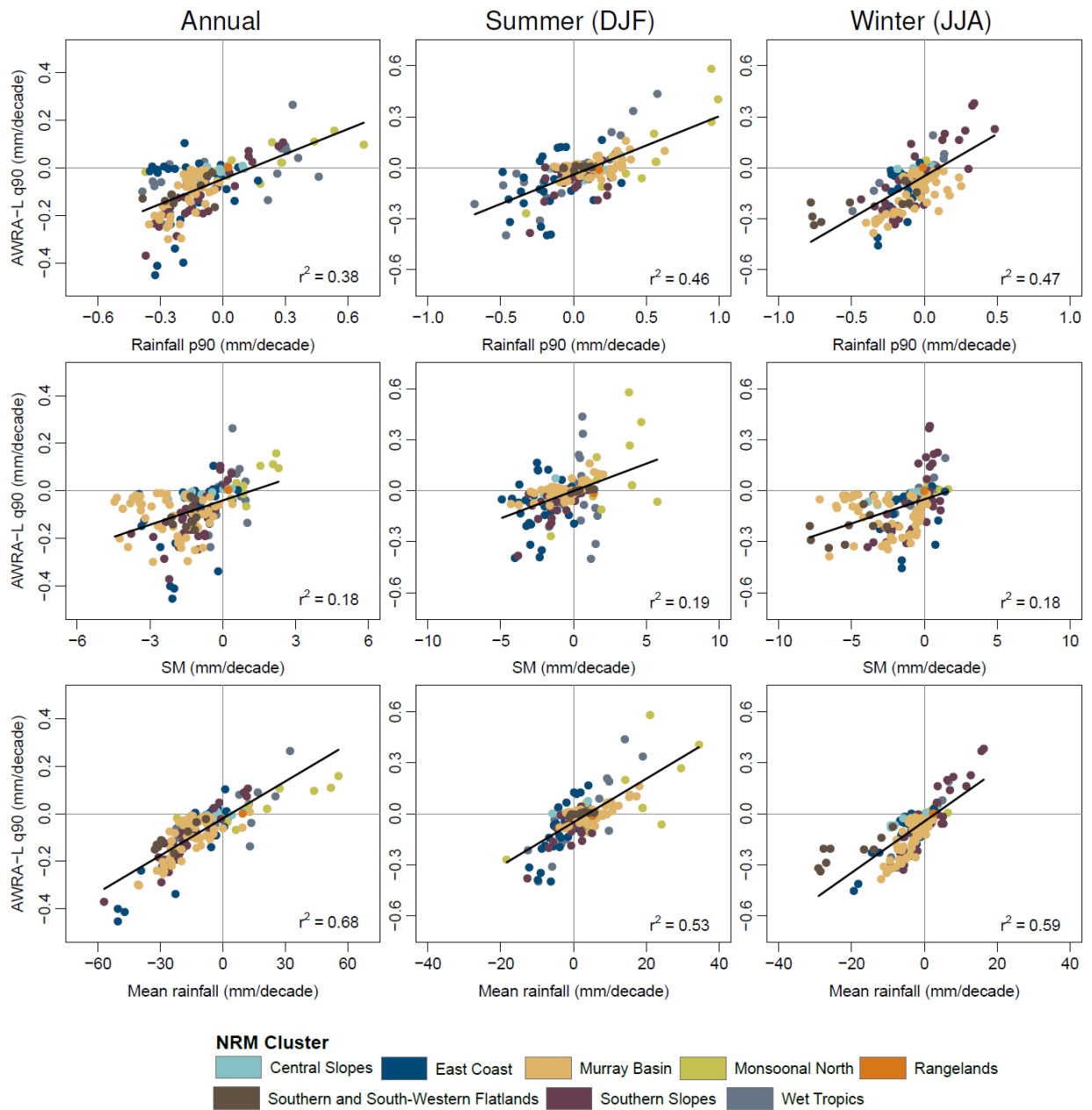
488 correspondence exists between soil moisture and runoff trends with r^2 values less than 0.1 (Table S1). The
489 East Coast and Central Slopes show strong positive annual associations between streamflow and soil
490 moisture of 0.34 and 0.57 respectively suggesting the east coast of Australia has a strong relationship with
491 soil moisture and runoff which was not present for the other variables. Although we can conclude that
492 rainfall changes are the dominant driver of changes in streamflow, soil moisture is a secondary driver with
493 the strength of the interaction between soil moisture and runoff varying strongly with season.

494 **3.6 Catchment scale interaction of hydroclimatological variables for high flows**

495 Figure 9 presents trends in the 90th percentile of annual catchment streamflow (q90) against the trends
496 in the 90th percentile of rainfall (p90), trends in soil moisture, and trends in mean rainfall from 1960 to
497 2017. Due to the small correlations of runoff trend to trends in PET and AET, and the shorter time scale of
498 high flows, the trends in PET and AET are omitted here. At an annual aggregation, the association between
499 q90 and p90 trends (0.38) is poorer than that of q90 with the mean rainfall (0.68). For each NRM region
500 the coefficient of determination is greater than 0.5 between q90 and mean rainfall (Table S2). There exists
501 variability between regions for the relationship between trends in q90 and p90 but in general the
502 strongest relationships exist between q90 and the mean rainfall (compared to p90 or soil moisture).

503 Seasonally, a strong relationship exists between trends in q90 and p90 across most regions. The
504 relationship between the trends in q90 and p90 appears weaker than the correlation between the trends
505 for mean rainfall and mean streamflow presented in Figure 8. This could be expected due to greater
506 variability in the more extreme flows and rainfalls, compared to mean flows and rainfalls. There is a weak
507 relationship between q90 and p90 trends in summer (DJF) for the Southern and South-Western Flatlands
508 and Southern Slopes (< 0.1), possibly due to the fact that this is not the dominant streamflow season, and
509 streamflow is baseflow dominated, resulting in higher associations with soil moisture (Table S2) up to
510 0.65 for the Southern and South-Western Flatlands .

511



513

514 **Figure 9.** Modelled q90 streamflow runoff trend per decade for 160 catchments across Australia against
 515 p90 rainfall, soil moisture (SM), and mean rainfall. Results are presented annually, for the austral
 516 summer months (DJF), and the austral winter (JJA). Catchment locations are shown in Figure 2. The black
 517 line is a line of best fit with the coefficient of determination (r^2) for each panel. Table S2 presents
 518 coefficients of determination for individual NRM regions.

519 There are quite large positive and negative trends in the Wet Tropics: q90 runoff with a strong association
520 to p90, up to 0.73 in the Wet Tropics for the summer season. In the Monsoonal North q90 is generally
521 increasing with increasing p90 (r^2 of 0.78). This is consistent with significant infiltration excess dominated
522 high flows during the monsoonal wet (DJF) season. For winter (JJA), the strongest positive trends in q90
523 are observed in the Southern Slopes, and the strongest negative trends in the Southern and South-
524 Western Flatlands, with an r^2 with the p90 trends of 0.67 and 0.55 respectively. The contrast to the
525 summer trends in this region being dominated by soil moisture changes demonstrates how changing high
526 (q90) runoff, as compared to mean runoff, is more linked to seasonality changes, and changes in seasonal
527 extremes may not necessarily translate to change in the annual mean. For example, for the Murray Basin
528 and Southern and South-Western Flatlands the summer association with soil moisture is greater than that
529 with p90. Comparing an r^2 of 0.65 for the South and South-Western Flatlands between q90 and soil
530 moisture with an r^2 of 0.09 for q90 and p90 demonstrates two points: first, high flows in seasons of low
531 rainfall are more related to soil moisture changes than extreme rainfall changes; second, seasonal changes
532 in high flows, out of sync with the maximum seasonality of flow, are dominant in this region. To
533 summarise, for the Murray Basin and Southern and South-Western Flatlands, soil moisture and the mean
534 climate state have a greater impact on changing high flows than changes in extreme rainfall.

535 Overall, the greatest association for trends in q90 is with trends in mean annual rainfall (Table S2). This
536 doesn't necessarily imply that mean rainfall changes are driving high flow changes, but, as extreme rainfall
537 changes constitute a large part of the volume of mean rainfall, we know that mean rainfall changes are
538 highly dependent on changes in extreme rainfall. Moreover, mean rainfall changes are a larger driver of
539 changes in soil moisture. Hence the trends in p90 rainfall and soil moisture are integrated into changes in
540 the mean rainfall and the association between q90 and mean rainfall trends (Figure 9) is similar to the
541 association between mean runoff and mean rainfall (Figure 8). Trends in q90 are similar to trends in mean
542 runoff confirming that the direction (positive or negative) of trend in the entire runoff distribution is the
543 same.

544 **4 Discussions and Conclusions**

545 We presented the first high-resolution evaluation of trends in key hydroclimatic variables across the
546 terrestrial water balance for the Australian continent. Compared to the gauging network of (daily) rainfall
547 observations, other hydrological variables such as evaporation, soil moisture, and streamflow (not
548 affected by human interaction/management) are much more sparsely measured, meaning most studies
549 of hydroclimatic trends are limited to rainfall and infer impacts to other parts of the water cycle from the

550 rainfall trends (e.g. Gallant et al., 2007). However, inferring trends in streamflow from rainfall alone can
551 be problematic due to the complex interactions present at catchment scale (e.g. Sharma et al., 2018).
552 Because of this, to quantify and understand changes in the hydrologic cycle both on the continental scale,
553 and in ungauged catchments, modelling is required. Here, we used the Australian Water Resource
554 Assessment model (AWRA-L) to study trends in rainfall, evapotranspiration, soil moisture, and runoff, as
555 well as indicators of flooding and drought across the continent.

556 **4.1 Evaluation of AWRA-L**

557 AWRA-L has been extensively evaluated for its performance in simulating soil moisture and runoff,
558 indicating its suitability for national water balance studies. We additionally evaluated the performance of
559 AWRA-L to simulate trends in catchment aggregated runoff, that is, the streamflow. Simulated annual
560 flow direction matched observations at 76% of the catchments with a coefficient of determination 0.38,
561 indicating good performance across the continent. Localised decreases in observed streamflow along the
562 north-east coast and at the very far south-west tip of the continent may be due to the fact that there is
563 one set of parameters applied nationally with local behaviour modulated according to input static grids of
564 landscape characteristics. This approach inevitably leads to areas where performance and behaviour does
565 not follow observed data (due to input uncertainties and errors along with poor local parameterisation).
566 However, as the performance of AWRA-L in ungauged basins approaches that of locally calibrated models
567 for streamflow, this gives confidence in the use of AWRA-L nationally (Frost and Wright, 2018)

568 Overall, good correspondence with observed trends was found in the south-east of Australia, in particular
569 in the Murray Basin and Southern Slopes NRM regions where observed drying trends are the largest.
570 Reasonable correspondence between modelled and observed trends in streamflow was found in the
571 northern parts of Australia for the warmer months when streamflow is greatest but on an annual basis,
572 the coefficient of determination was less than 0.1 in the tropics. The large variability in the magnitude of
573 the modelled trend in the tropics may be in part due to drainage currently being overly dependent on
574 saturated conductivity, and not enough on rainfall variability in the gridded rainfall driving the model. But
575 it should also be noted that this region generally has catchments which are larger in area and ephemeral
576 leading to greater variability in observed trends.

577 **4.2 Trends in hydroclimatic variables across Australia**

578 Linear trends show that, consistent with the tropics expanding poleward (Grise et al., 2018; Staten et al.,
579 2018), there has been increasing precipitation in the tropics and decreasing precipitation in the sub-

580 tropics, with trends to wetter conditions in the monsoon-dominated summer months in the north and
581 drier conditions in the south in the winter months. As changes in rainfall corresponds to the dominant
582 rainfall seasonality for Australia, on a continental scale there is correspondence between the trends in
583 rainfall, AET, soil moisture and runoff since 1960. There is little correspondence between PET and AET
584 trends with the primary (only) exception some limited regions on the south-east coast. The divergence of
585 PET and AET trends fits with the fact that Australia as a whole is a moisture limited environment (Anabalón
586 and Sharma, 2017).

587 Consistent with extreme rainfalls (by volume) contributing most to the mean rainfall distribution
588 (Taschetto and England, 2009; Wasko and Nathan, 2019b) and the entire flow distribution trending in the
589 same direction with climate change (Gudmundsson et al., 2019), trends in the 90th percentile of runoff are
590 largely related to changes in mean rainfall. Decreases in high flows (an indicator of flooding) are the
591 greatest in the south-west and south-east coastal regions of Australia. But more severe flow extremes,
592 such as the 5day annual maxima flow, exhibit less negative trends, suggesting the more extreme the flow
593 event, the more likely it is to be increasing (Wasko and Nathan, 2019a).

594 Indicators of drought suggest a shift to more frequent occurrences (and more widespread) drought across
595 large parts of Australia. Although shifts to more frequent drought conditions are largely contained to the
596 Southern Slopes, South and South-Western Flatlands, and Murray Basin, there is evidence that parts of
597 the tropics will also experience increasing drought, despite increases in rainfall. Although the eastern half
598 of the Southern and South-Western Flatlands did not exhibit strong trends in decreasing runoff, there was
599 a large decrease in the SRI-12 indicating a shift to more drought conditions. This is consistent with
600 increasing variability in rainfall (Rajah et al., 2014) rather than changes in total mean rainfall causing
601 greater restrictions to seasonal water supply (Nguyen et al., 2020).

602 Despite strong visual correlation between trends in rainfall, soil moisture, evapotranspiration and runoff
603 at the continental scale, annual streamflow trends at the regional scale show the greatest association to
604 rainfall trends with an r^2 of 0.74. This suggests rainfall changes are driving changes in streamflow and soil
605 moisture is a secondary driver (r^2 of 0.23 annually). In the dry summer months, the associations of runoff
606 and soil moisture (r^2 of 0.40) for the Murray Basin are similar to that between runoff and rainfall (r^2 of
607 0.49). This presents that soil moisture changes are a secondary driver of streamflow trends, except in dry
608 months, where soil moisture is equally a primary driver.

609 For the 90th percentile of streamflow, trends were more closely aligned to mean rainfall changes (r^2 of
610 0.68) rather than the 90th percentile of rainfall (r^2 of 0.38). As extreme rainfall changes constitute a large
611 part of the volume of mean rainfall change, the 90th percentile of rainfall and soil moisture are integrated
612 into changes in mean rainfall. This suggests that trends in high flows are modulated by both rainfall and
613 soil moisture changes. Indeed for the dry summer months in the Murray Basin and Southern and South-
614 Western Flatlands, the association with soil moisture is greater than that with p90, indicating how high
615 flows in seasons of low rainfall are more related to changes in soil moisture than extreme rainfall changes,
616 with the converse true for the high rainfall season.

617 **4.3 Implications and future work**

618 Here we successfully performed a trend analysis of key hydrologic variables from 1960 to 2017 using
619 continental scale water balance model (AWRA-L). We found trends towards greater rainfalls and water
620 availability in the tropics with declines in rainfall and water availability in the south of the continent. While
621 there is evidence of increasing extreme rainfalls across Australia, annual maxima flooding has decreased
622 across large parts of the country. Declining rainfalls and streamflow in southeast Australia have resulted in
623 increasing droughts affecting agriculture and water supply and if these trends are to continue, we can
624 expect consequences to be further exacerbated.

625 Future work will focus on better understanding the impacts of climate change on water supply across
626 Australia and the impact of changes in seasonality on drought and flooding. Localised projections of the
627 impacts of changing hydrologic conditions on water supply exist for Australia (Henley et al., 2019; Nguyen
628 et al., 2020), but we envisage that projections of AWRA-L will enable the development of more extensive
629 studies that lead to greater understanding and a more holistic picture of the impacts of climate change
630 on flooding and water supply across Australia.

631 **Acknowledgements**

632 Conrad Wasko receives funding from the University of Melbourne McKenzie Postdoctoral Fellowship
633 scheme and Australian Research Council (ARC) Discovery Project DP200101326.

634 **References**

635 Albergel, C., Dorigo, W., Reichle, R.H., Balsamo, G., de Rosnay, P., Muñoz-Sabater, J., Isaksen, L., de Jeu,
636 R., Wagner, W., 2013. Skill and Global Trend Analysis of Soil Moisture from Reanalyses and
637 Microwave Remote Sensing. *J. Hydrometeorol.* 14, 1259–1277. <https://doi.org/10.1175/JHM-D-12->

638 0161.1

639 Alexander, L.V., Hope, P., Collins, D., Trewin, B., Lynch, A., Nicholls, N., 2007. Trends in Australia's
640 climate means and extremes: a global context. *Aust. Meteorol. Mag.* 56, 1–18.
641 <https://doi.org/10.1029/2005JD006119>Alexander

642 Alexander, L. V., Arblaster, J.M., 2017. Historical and projected trends in temperature and precipitation
643 extremes in Australia in observations and CMIP5. *Weather Clim. Extrem.* 15, 34–56.
644 <https://doi.org/10.1016/j.wace.2017.02.001>

645 Allan, R.P., Barlow, M., Byrne, M.P., Cherchi, A., Douville, H., Fowler, H.J., Gan, T.Y., Pendergrass, A.G.,
646 Rosenfeld, D., Swann, A.L.S., Wilcox, L.J., 2020. Advances in understanding large-scale responses of
647 the water cycle to climate change. *Ann. N. Y. Acad. Sci.* 1–27. <https://doi.org/10.1111/nyas.14337>

648 Allen, M.R., Ingram, W.J., 2002. Constraints on future changes in climate and the hydrologic cycle.
649 *Nature* 419, 224–232. <https://doi.org/10.1038/nature01092>

650 Anabalón, A., Sharma, A., 2017. On the divergence of potential and actual evapotranspiration trends: An
651 assessment across alternate global datasets. *Earth's Futur.* 5, 905–917.
652 <https://doi.org/10.1002/2016EF000499>

653 Andersson, J.C.M., Pechlivanidis, I.G., Gustafsson, D., Donnelly, C., Arheimer, B., 2015. Key factors for
654 improving large-scale hydrological model performance. *Eur. Water* 49, 77–88.

655 Asadi Zarch, M.A., Sivakumar, B., Sharma, A., 2015. Droughts in a warming climate: A global assessment
656 of Standardized precipitation index (SPI) and Reconnaissance drought index (RDI). *J. Hydrol.* 526,
657 183–195. <https://doi.org/10.1016/j.jhydrol.2014.09.071>

658 Ball, J., Babister, M., Nathan, R., Weeks, W., Wienmann, R., Retallick, M., Testoni, I. (Eds.), 2019.
659 *Australian Rainfall and Runoff: A Guide to Flood Estimation.* Commonwealth of Australia.

660 Beck, H.E., Wood, E.F., Pan, M., Fisher, C.K., Miralles, D.G., van Dijk, A.I.J.M., McVicar, T.R., Adler, R.F.,
661 2019. MSWEP V2 Global 3-Hourly 0.1° Precipitation: Methodology and Quantitative Assessment.
662 *Bull. Am. Meteorol. Soc.* 100, 473–500. <https://doi.org/10.1175/BAMS-D-17-0138.1>

663 Becker, A., Finger, P., Meyer-Christoffer, A., Rudolf, B., Schamm, K., Schneider, U., Ziese, M., 2013. A
664 description of the global land-surface precipitation data products of the Global Precipitation
665 Climatology Centre with sample applications including centennial (trend) analysis from 1901-

666 present. *Earth Syst. Sci. Data* 5, 71–99. <https://doi.org/10.5194/essd-5-71-2013>

667 Berghuijs, W.R., Harrigan, S., Molnar, P., Slater, L.J., Kirchner, J.W., 2019. The Relative Importance of
668 Different Flood-Generating Mechanisms Across Europe. *Water Resour. Res.* 2019WR024841.
669 <https://doi.org/10.1029/2019WR024841>

670 Chiew, F.H.S., McMahon, T.A., 2002. Global ENSO-streamflow teleconnection, streamflow forecasting
671 and interannual variability. *Hydrol. Sci. J.* 47, 505–522.
672 <https://doi.org/10.1080/02626660209492950>

673 CSIRO & BOM, 2018. *State of the Climate*.

674 CSIRO, Bureau of Meteorology, 2015. *Climate Change in Australia Projections for Australia’s Natural
675 Resource Management Regions: Technical Report*.

676 Dey, R., Gallant, A.J.E., Lewis, S.C., 2020. Evidence of a continent-wide shift of episodic rainfall in
677 Australia. *Weather Clim. Extrem.* 29, 100274. <https://doi.org/10.1016/j.wace.2020.100274>

678 Dey, R., Lewis, S.C., Arblaster, J.M., Abram, N.J., 2019. A review of past and projected changes in
679 Australia’s rainfall. *Wiley Interdiscip. Rev. Clim. Chang.* 10, 1–23. <https://doi.org/10.1002/wcc.577>

680 Do, H.X., Westra, S., Leonard, M., 2017. A global-scale investigation of trends in annual maximum
681 streamflow. *J. Hydrol.* 552, 28–43. <https://doi.org/10.1016/j.jhydrol.2017.06.015>

682 Donat, M.G., Alexander, L. V., Yang, H., Durre, I., Vose, R., Dunn, R.J.H., Willett, K.M., Aguilar, E., Brunet,
683 M., Caesar, J., Hewitson, B., Jack, C., Klein Tank, a. M.G., Kruger, a. C., Marengo, J., Peterson, T.C.,
684 Renom, M., Oria Rojas, C., Rusticucci, M., Salinger, J., Elayah, a. S., Sekele, S.S., Srivastava, a. K.,
685 Trewin, B., Villarreal, C., Vincent, L. a., Zhai, P., Zhang, X., Kitching, S., 2013. Updated analyses of
686 temperature and precipitation extreme indices since the beginning of the twentieth century: The
687 HadEX2 dataset. *J. Geophys. Res. Atmos.* 118, 2098–2118. <https://doi.org/10.1002/jgrd.50150>

688 Donohue, R.J., McVicar, T.R., Roderick, M.L., 2010. Assessing the ability of potential evaporation
689 formulations to capture the dynamics in evaporative demand within a changing climate. *J. Hydrol.*
690 386, 186–197.

691 Elmahdi, A., Hafeez, M., Smith, A., Frost, A., 2016. Using an integrated continental hydrological model
692 (AWRA modelling system) to inform Australian water resources assessment, in: 37th Hydrology and
693 Water Resources Symposium 2016: Water, Infrastructure and the Environment, HWRS 2016.

694 Fawcett, R., Trewin, B.C., Braganza, K., Smalley, R.J., Jovanovic, B., Jones, D.A., 2012. On the sensitivity of
695 Australian temperature trends and variability to analysis methods and observation networks,
696 CAWCR Technical Report No. 050.

697 Feng, H., Zhang, M., 2015. Global land moisture trends: Drier in dry and wetter in wet over land. *Sci.*
698 *Rep.* 5, 1–6. <https://doi.org/10.1038/srep18018>

699 Fowler, K.J.A., Peel, M.C., Western, A.W., Zhang, L., Peterson, T.J., 2016. Simulating runoff under
700 changing climatic conditions: Revisiting an apparent deficiency of conceptual rainfall-runoff
701 models. *Water Resour. Res.* 52, 1820–1846. <https://doi.org/10.1002/2015WR018068>

702 Frost, A.J., Ramchurn, A., Smith, A., 2018. The Australian landscape water balance model (AWRA-L v6).
703 Technical Description of the Australian Water Resources Assessment Landscape model version 6.
704 Melbourne, Australia.

705 Frost, A.J., Wright, D.P., 2018. Evaluation of the Australian Landscape Water Balance model (AWRA-L
706 v6): Comparison of AWRA-L v6 against Observed Hydrological Data and Peer Models.

707 Frost, Andrew J., Wright, D.P., 2018. Evaluation of the Australian Landscape Water Balance model :
708 AWRA-L v6. A comparison of AWRA-L v6 against Observed Hydrological Data and Peer Models.
709 Melbourne, Australia.

710 Gallant, A.J.E., Hennessy, K.J., Risbey, J., 2007. Trends in rainfall indices for six Australian regions: 1910-
711 2005. *Aust. Meteorol. Mag.* 56, 223–239.

712 Grant, I., Jones, D., Wang, W., Fawcett, R., Barratt, D., 2008. Meteorological and remotely sensed
713 datasets for hydrological modelling: a contribution to the Australian Water Availability Project, in:
714 Catchment-Scale Hydrological Modelling and Data Assimilation (CAHMDA-3) International
715 Workshop on Hydrological Prediction: Modelling, Observation and Data Assimilation. Melbourne,
716 Australia.

717 Grise, K.M., Davis, S.M., Staten, P.W., Adam, O., 2018. Regional and seasonal characteristics of the
718 recent expansion of the tropics. *J. Clim.* 31, 6839–6856. <https://doi.org/10.1175/JCLI-D-18-0060.1>

719 Groisman, P.Y., Knight, R.W., Easterling, D.R., Karl, T.R., Hegerl, G.C., Razuvaev, V.N., 2005. Trends in
720 Intense Precipitation in the Climate Record. *J. Clim.* 18, 1326–1350.
721 <https://doi.org/10.1175/JCLI3339.1>

722 Gudmundsson, L., Leonard, M., Do, H.X., Westra, S., Seneviratne, S.I., 2019. Observed Trends in Global
723 Indicators of Mean and Extreme Streamflow. *Geophys. Res. Lett.* 46, 756–766.
724 <https://doi.org/10.1029/2018GL079725>

725 Guerreiro, S.B., Fowler, H.J., Barbero, R., Westra, S., Lenderink, G., Blenkinsop, S., Lewis, E., Li, X.-F.,
726 2018. Detection of continental-scale intensification of hourly rainfall extremes. *Nat. Clim. Chang.* 8,
727 803–807. <https://doi.org/10.1038/s41558-018-0245-3>

728 Hafeez, M., Smith, A., Frost, A., Srikanthan, R., Barua, S., Elmahdi, A., 2015. The Bureau’s Operational
729 Australian Water Resources Assessment Modelling System (AWRAMS): From Science to End Users
730 Applications and Future Directions, in: *Modsim 2015 21st International Congress on Modelling and*
731 *Simulation.*

732 Hartmann, D.L., Klein Tank, A.M.G., Rusticucci, M., Alexander, L. V., Broennimann, S., Charabi, Y.,
733 Dentener, F.J., Dlugokencky, E.J., Easterling, D.R., Kaplan, A., Soden, B.J., Thorne, P.W., Wild, M.,
734 Zhai, P.M., 2013. Observations: Atmosphere and Surface, in: Stocker, T., Qin, D., Plattner, G.-K.,
735 Tignor, M., Allen, S.K., Boschung, J., Nauels, A., Xia, Y., Bex, V., Midgley, P.M. (Eds.), *Climate Change*
736 *2013: The Physical Science Basis. Contribution of Working Group I to the Fifth Assessment Report*
737 *of the Intergovernmental Panel on Climate Change.* Cambridge University Press, Cambridge, UK
738 and New York, NY, USA, pp. 159–254.

739 Henley, B.J., Peel, M.C., Nathan, R., King, A.D., Ukkola, A.M., Karoly, D.J., Tan, K.S., 2019. Amplification of
740 risks to water supply at 1.5 °C and 2 °C in drying climates: a case study for Melbourne, Australia.
741 *Environ. Res. Lett.* 14, 084028. <https://doi.org/10.1088/1748-9326/ab26ef>

742 Hill, P., Thomson, R., 2019. Chapter 3. Losses, Book 5: Flood Hydrograph Estimation:, in: Ball, J., Babister,
743 M., Nathan, R., Weinmann, E., Retallick, M., Testoni, I. (Eds.), *Australian Rainfall and Runoff - A*
744 *Guide to Flood Estimation.* Commonwealth of Australia.

745 Hill, P., Zhang, J., Nathan, R., 2016. Australian rainfall and runoff Revision Project 6: Loss models for
746 catchment simulation. Barton, ACT.

747 Holgate, C., De Jeu, R.A.M., van Dijk, A.I.J., Liu, Y., Renzullo, L.J., Vinodkumar, Dharssi, I., Parinussa,
748 R.M., Van Der Schalie, R., Gevaert, A., Walker, J., McJannet, D., Cleverly, J., Haverd, V., Trudinger,
749 C.M., Briggs, P.R., 2016. Comparison of remotely sensed and modelled soil moisture data sets
750 across Australia. *Remote Sens. Environ.* 186, 479–500. <https://doi.org/10.1016/j.rse.2016.09.015>

751 Huntington, T.G., 2006. Evidence for intensification of the global water cycle: Review and synthesis. *J.*
752 *Hydrol.* 319, 83–95. <https://doi.org/10.1016/j.jhydrol.2005.07.003>

753 Ishak, E.H., Rahman, A., Westra, S., Sharma, A., Kuczera, G., 2013. Evaluating the non-stationarity of
754 Australian annual maximum flood. *J. Hydrol.* 494, 134–145.
755 <https://doi.org/10.1016/j.jhydrol.2013.04.021>

756 Ivancic, T.J., Shaw, S.B., 2015. Examining why trends in very heavy precipitation should not be mistaken
757 for trends in very high river discharge. *Clim. Change* 133, 681–693.
758 <https://doi.org/10.1007/s10584-015-1476-1>

759 Johnson, F., Sharma, A., 2010. A Comparison of Australian Open Water Body Evaporation Trends for
760 Current and Future Climates Estimated from Class A Evaporation Pans and General Circulation
761 Models. *J. Hydrometeorol.* 11, 105–121. <https://doi.org/10.1175/2009JHM1158.1>

762 Johnson, F., White, C.J., van Dijk, A., Ekstrom, M., Evans, J.P., Jakob, D., Kiem, A.S., Leonard, M.,
763 Rouillard, A., Westra, S., 2016. Natural hazards in Australia: floods. *Clim. Change* 139, 21–35.
764 <https://doi.org/10.1007/s10584-016-1689-y>

765 Jones, D., Wang, W., Fawcett, R., 2009. High-quality spatial climate data-sets for Australia. *Aust.*
766 *Meteorol. Oceanogr. J.* 58, 233–248.

767 Jung, M., Reichstein, M., Ciais, P., Seneviratne, S.I., Sheffield, J., Goulden, M.L., Bonan, G., Cescatti, A.,
768 Chen, J., de Jeu, R., Dolman, A.J., Eugster, W., Gerten, D., Gianelle, D., Gobron, N., Heinke, J.,
769 Kimball, J., Law, B.E., Montagnani, L., Mu, Q., Mueller, B., Oleson, K., Papale, D., Richardson, A.D.,
770 Roupsard, O., Running, S., Tomelleri, E., Viovy, N., Weber, U., Williams, C., Wood, E., Zaehle, S.,
771 Zhang, K., 2010. Recent decline in the global land evapotranspiration trend due to limited moisture
772 supply. *Nature* 467, 951–954. <https://doi.org/10.1038/nature09396>

773 Kharin, V. V., Zwiers, F.W., Zhang, X., Wehner, M., 2013. Changes in temperature and precipitation
774 extremes in the CMIP5 ensemble. *Clim. Change* 119, 345–357. [https://doi.org/10.1007/s10584-](https://doi.org/10.1007/s10584-013-0705-8)
775 [013-0705-8](https://doi.org/10.1007/s10584-013-0705-8)

776 Kiem, A.S., Johnson, F., Westra, S., van Dijk, A., Evans, J.P., O'Connell, A., Rouillard, A., Barr, C., Tyler,
777 J., Thyer, M., Jakob, D., Woldemeskel, F., Sivakumar, B., Mehrotra, R., 2016. Natural hazards in
778 Australia: droughts. *Clim. Change* 139, 37–54. <https://doi.org/10.1007/s10584-016-1798-7>

779 King, A.D., Pitman, A.J., Henley, B.J., Ukkola, A.M., Brown, J.R., 2020. The role of climate variability in
780 Australian drought. *Nat. Clim. Chang.* 10, 177–179. <https://doi.org/10.1038/s41558-020-0718-z>

781 Kirono, D.G.C., Hennessy, K.J., Grose, M.R., 2017. Increasing risk of months with low rainfall and high
782 temperature in southeast Australia for the past 150 years. *Clim. Risk Manag.* 16, 10–21.
783 <https://doi.org/10.1016/j.crm.2017.04.001>

784 Koutsoyiannis, D., 2020. Revisiting the global hydrological cycle: is it intensifying? *Hydrol. Earth Syst. Sci.*
785 24, 3899–3932. <https://doi.org/10.5194/hess-24-3899-2020>

786 Liu, Y., Liu, Y., Wang, W., 2019. Inter-comparison of satellite-retrieved and Global Land Data Assimilation
787 System-simulated soil moisture datasets for global drought analysis. *Remote Sens. Environ.* 220, 1–
788 18. <https://doi.org/10.1016/j.rse.2018.10.026>

789 Martinez-Villalobos, C., Neelin, J.D., 2018. Shifts in Precipitation Accumulation Extremes During the
790 Warm Season Over the United States. *Geophys. Res. Lett.* 45, 8586–8595.
791 <https://doi.org/10.1029/2018GL078465>

792 McKee, T.B., Doesken, N.J., Kleist, J., 1993. The relationship of drought frequency and duration to time
793 scales, in: Eighth Conference on Applied Climatology. Anaheim, California.
794 <https://doi.org/10.1002/jso.23002>

795 McMahan, T.A., Vogel, R.M., Peel, M.C., Pegram, G.G.S., 2007. Global streamflows - Part 1:
796 Characteristics of annual streamflows. *J. Hydrol.* 347, 243–259.
797 <https://doi.org/10.1016/j.jhydrol.2007.09.002>

798 McVicar, T.R., Van Niel, T.G., Li, L.T., Roderick, M.L., Rayner, D.P., Ricciardulli, L., Donohue, R.J., 2008.
799 Wind speed climatology and trends for Australia, 1975-2006: Capturing the stilling phenomenon
800 and comparison with near-surface reanalysis output. *Geophys. Res. Lett.* 35, 1–6.
801 <https://doi.org/10.1029/2008GL035627>

802 Nathan, R.J., McMahan, T.A., Peel, M.C., Horne, A., 2019. Assessing the degree of hydrologic stress due
803 to climate change. *Clim. Change* 156, 87–104. <https://doi.org/10.1007/s10584-019-02497-4>

804 Nguyen, H., Mehrotra, R., Sharma, A., 2020. Assessment of climate change impacts on reservoir storage
805 reliability, resilience and vulnerability using a Multivariate Frequency Bias Correction approach.
806 *Water Resour. Res.* 0–3. <https://doi.org/10.1029/2019wr026022>

807 Nguyen, H., Wheeler, M.C., Otkin, J.A., Cowan, T., Frost, A., Stone, R., 2019. Using the evaporative stress
808 index to monitor flash drought in Australia. *Environ. Res. Lett.* 14. [https://doi.org/10.1088/1748-](https://doi.org/10.1088/1748-9326/ab2103)
809 [9326/ab2103](https://doi.org/10.1088/1748-9326/ab2103)

810 Peel, M.C., McMahon, T.A., Finlayson, B.L., 2004. Continental differences in the variability of annual
811 runoff-update and reassessment. *J. Hydrol.* 295, 185–197.
812 <https://doi.org/10.1016/j.jhydrol.2004.03.004>

813 Penman, H.L., 1948. Natural Evaporation from Open Water, Bare Soil and Grass. *R. Soc.* 193, 120–145.
814 <https://doi.org/10.1098/rspa.1948.0037>

815 Peterson, T.J., Wasko, C., Saft, M., Peel, M.C., 2020. AWAPer: An R package for area weighted catchment
816 daily meteorological data anywhere within Australia. *Hydrol. Process.* 34, 1301–1306.
817 <https://doi.org/10.1002/hyp.13637>

818 Potter, N.J., Chiew, F.H.S., Frost, A.J., 2010. An assessment of the severity of recent reductions in rainfall
819 and runoff in the Murray-Darling Basin. *J. Hydrol.* 381, 52–64.
820 <https://doi.org/10.1016/j.jhydrol.2009.11.025>

821 Rajah, K., O’Leary, T., Turner, A., Petrakis, G., Leonard, M., Westra, S., 2014. Changes to the temporal
822 distribution of daily precipitation. *Geophys. Res. Lett.* 41, 8887–8894.
823 <https://doi.org/10.1002/2014GL062156>

824 Risbey, J.S., Pook, M.J., McIntosh, P.C., 2013. Spatial trends in synoptic rainfall in southern Australia.
825 *Geophys. Res. Lett.* 40, 3781–3785. <https://doi.org/10.1002/grl.50739>

826 Saft, M., Peel, M.C., Western, A.W., Zhang, L., 2016. Predicting shifts in rainfall-runoff partitioning during
827 multiyear drought: Roles of dry period and catchment characteristics. *Water Resour. Res.* 52,
828 9290–9305. <https://doi.org/10.1002/2016WR019525>

829 Saft, M., Western, A.W., Zhang, L., Peel, M.C., Potter, N.J., 2015. The influence of multiyear drought on
830 the annual rainfall-runoff relationship: An Australian perspective. *Water Resour. Res.* 51, 2444–
831 2463. <https://doi.org/10.1002/2014WR015348>

832 Sharma, A., Wasko, C., Lettenmaier, D.P., 2018. If Precipitation Extremes Are Increasing, Why Aren’t
833 Floods? *Water Resour. Res.* 54, 8545–8551. <https://doi.org/10.1029/2018WR023749>

834 Shukla, S., Wood, A.W., 2008. Use of a standardized runoff index for characterizing hydrologic drought.

835 Geophys. Res. Lett. 35, 1–7. <https://doi.org/10.1029/2007GL032487>

836 Staten, P.W., Lu, J., Grise, K.M., Davis, S.M., Birner, T., 2018. Re-examining tropical expansion. *Nat. Clim.*
837 *Chang.* 8, 768–775. <https://doi.org/10.1038/s41558-018-0246-2>

838 Stephens, C.M., McVicar, T.R., Johnson, F.M., Marshall, L.A., 2018. Revisiting Pan Evaporation Trends in
839 Australia a Decade on. *Geophys. Res. Lett.* 45, 11,164–11,172.
840 <https://doi.org/10.1029/2018GL079332>

841 Sun, Q., Zhang, X., Zwiers, F., Westra, S., Alexander, L. V., 2020. A global, continental and regional
842 analysis of changes in extreme precipitation. *J. Clim.* 1–52. [https://doi.org/10.1175/JCLI-D-19-](https://doi.org/10.1175/JCLI-D-19-0892.1)
843 [0892.1](https://doi.org/10.1175/JCLI-D-19-0892.1)

844 Taschetto, A.S., England, M.H., 2009. An analysis of late twentieth century trends in Australian rainfall.
845 *Int. J. Climatol.* 29, 791–807. <https://doi.org/10.1002/joc.1736>

846 Trambly, Y., Mimeau, L., Neppel, L., Vinet, F., Sauquet, E., 2019. Detection and attribution of flood
847 trends in Mediterranean basins. *Hydrol. Earth Syst. Sci.* 23, 4419–4431.
848 <https://doi.org/10.5194/hess-23-4419-2019>

849 Van Dijk, A., 2010. The Australian Water Resources Assessment System. Technical Report 3. Landscape
850 Model (version 0.5) Technical Description. CSIRO: Water for a Healthy Country National Research
851 Flagship.

852 Van Dijk, A.I.J.M., Beck, H.E., Crosbie, R.S., De Jeu, R.A.M., Liu, Y.Y., Podger, G.M., Timbal, B., Viney, N.R.,
853 2013. The Millennium Drought in southeast Australia (2001–2009): Natural and human causes and
854 implications for water resources, ecosystems, economy, and society. *Water Resour. Res.* 49, 1040–
855 1057. <https://doi.org/10.1002/wrcr.20123>

856 Viney, N., Vaze, J., Crosbie, R., Wang, B., Dawes, W., Frost, A., 2015. AWRA-L v5.0: technical description
857 of model algorithms and inputs. <https://doi.org/https://doi.org/10.4225/08/58518bc790ff7>

858 Wasko, C., Nathan, R., 2019a. Influence of changes in rainfall and soil moisture on trends in flooding. *J.*
859 *Hydrol.* 575, 432–441. <https://doi.org/10.1016/j.jhydrol.2019.05.054>

860 Wasko, C., Nathan, R., 2019b. The local dependency of precipitation on historical changes in
861 temperature. *Clim. Change* 156, 105–120. <https://doi.org/10.1007/s10584-019-02523-5>

862 Wasko, C., Nathan, R., Peel, M.C., 2020. Changes in Antecedent Soil Moisture Modulate Flood

863 Seasonality in a Changing Climate. *Water Resour. Res.* 56, e2019WR026300.
864 <https://doi.org/10.1029/2019WR026300>

865 Wasko, C., Sharma, A., Lettenmaier, D.P., 2019. Increases in temperature do not translate to increased
866 flooding. *Nat. Commun.* 10, 5676. <https://doi.org/10.1038/s41467-019-13612-5>

867 Weedon, G.P., Balsamo, G., Bellouin, N., Gomes, S., Best, M.J., Viterbo, P., 2014. Data methodology
868 applied to ERA-Interim reanalysis data. *Water Resour. Res.* 50, 7505–7514.
869 <https://doi.org/10.1002/2014WR015638>.Received

870 Westra, S., Alexander, L., Zwiers, F., 2013. Global increasing trends in annual maximum daily
871 precipitation. *J. Clim.* 26, 3904–3918. <https://doi.org/http://dx.doi.org/10.1175/JCLI-D-12-00502.1>

872 Whitfield, P.H., 2012. Floods in future climates: A review. *J. Flood Risk Manag.* 5, 336–365.
873 <https://doi.org/10.1111/j.1753-318X.2012.01150.x>

874 Zeng, Z., Peng, L., Piao, S., 2018. Response of terrestrial evapotranspiration to Earth’s greening. *Curr.*
875 *Opin. Environ. Sustain.* 33, 9–25. <https://doi.org/10.1016/j.cosust.2018.03.001>

876 Zhang, X.S., Amirthanathan, G.E., Bari, M.A., Laugesen, R.M., Shin, D., Kent, D.M., MacDonald, A.M.,
877 Turner, M.E., Tuteja, N.K., 2016. How streamflow has changed across Australia since the 1950s:
878 evidence from the network of hydrologic reference stations. *Hydrol. Earth Syst. Sci.* 20, 3947–3965.
879 <https://doi.org/10.5194/hess-20-3947-2016>

880 Zhang, Y.Q., Viney, N., Chen, Y., Li, H.Y., 2011. Collation of streamflow dataset for 719 unregulated
881 Australian catchments. CSIRO: Water for a Healthy Country National Research Flagship.

882